NORMALIZED DIFFERENCE VEGETATIVE INDEX BASED CROP YIELD PREDICTION MODELS TO MINIMIZE NITROGEN FERTILIZER APPLICATION

By

Alvin Dean Monroe, Jr

Bachelor of Science in Cartography
East Central University
Ada, Oklahoma
1999

Master of Science in Geography
Oklahoma State University
Stillwater, Oklahoma
2001

Submitted to the Faculty of the
Graduate College of the
Oklahoma State University
in partial fulfillment of
the requirements for
the Degree of
DOCTOR OF PHILOSOPHY
December 2008

NORMALIZED DIFFERENCE VEGETATIVE INDEX

BASED CROP YIELD PREDICTION MODELS TO

MINIMIZE NITROGEN

FERTILIZER APPLICATION

Dissertation Approved:

Dr. John Solie

Dissertation Adviser

Dr. William Raun

Dr. Paul Weckler

Dr. Daniel Storm

Dr. Jonathan Comer

Dr. A. Gordon Emslie

Dean of the Graduate College

ACKNOWLEDGMENTS

The author wishes to acknowledge the kind and ever helpful physical support received from the staff Oklahoma State University Department of Biological and Agricultural Engineering, particularly Mrs. Jana Moore, Mrs. Nancy Rogers, and Mr. Craig Trible. The author also acknowledges the support of the Environmental Science Department, especially Mrs. Henderson, for her tireless efforts. Much appreciation goes to Mr. Tim Raczkowski (Northern Oklahoma College, Department of Mathematics) for editing and insight on the first generation of response equations.

Special thanks and much appreciation goes to my wife, Dr. Sierra Howry (Angelo State University), for her assistance in editing first drafts, listening to ideas, and her ever-helpful suggestions. Most especially, I want to thank her for support and encouragement through this process.

Thanks to my committee for attending and participating in the process of this dissertation and for a critical review of the findings. A special note of thanks to Dr. Jon Comer for enduring another of my committees.

A special thanks to Dr. John Solie for his mentorship as a researcher, patience as chair of my research committee, and encouragement as a friend. I very much enjoyed my time working with Dr. Solie and hope to someday teach as much to another as I learned from him.

TABLE OF CONTENTS

Chapter Page

LIST OF TABLES

Table Page

LIST OF FIGURES

Figure Page

Figure Page

CHAPTER I

INTRODUCTION

Commercial nitrogen (N) plays a significant role in sustaining cropping systems as a primary replacement nutrient. With each harvest, a portion of the native N is removed from the field and transported off-site reducing residual N for future crop use. Nitrogen, until recently, was a low cost supplement, which because of near universal limitation usually guarantees yield improvement over N depleted native stands. Low cost and significant yield improvement led to the wide scale N fertilizer use in uniform, usually high application rates as growing season insurance. However, application typically far exceeds necessity leading to vast quantities of residual N in the plant/soil matrix. Nitrogen, in most of its forms, is highly mobile, and is, accordingly, prone to off-site migration. Consequently, many years of over-application has elevated nitrate concentration in surface and sub-surface water supplies.

Nitrogen is a primary nutrient for algae; therefore, elevated N in water supplies can promote an elevated algal population, which over time builds detrital material, increases oxygen demand, and may prematurely age the water body. However, N is not typically the principal limiting factor in algal populations because of its high mobility; therefore, environmental concern about N usually revolves around human health issues from contamination of potable water.

Methemoglobinemia (blue baby syndrome), and a speculated linkage to non-Hodgkin's Lymphoma and digestive tract cancers have been cited as primary concerns for N ingestion. However, in many cases concentration of N in water supply is lower than regulatory standards, and has not risen to popular concern as demonstrated in a lack of literature citing direct causal effects; however, current research suggest that aqueous forms of N leaching into natural waterways can lead to aquatic fauna mortality.

Off-site N migration is of particular concern economically because it represents lost opportunity to the farmer. As petroleum prices increase, N fertilizer price, contingent on the price of natural gas, will commensurately increase. Agricultural profitability, especially with competition on the world market and rising petroleum prices, is becoming a matter of cost reduction through efficient application. Additionally, efficient N application to meet cost-reducing strategies has the potential of creating positive externalities for the environment without regulatory action.

To address need and maximize yield several issues must be considered in applying supplemental N. At the individual plant level there must be enough fertilizer N to minimize the disparity between residual N in the plant/soil matrix and the optimum plant capacity for N uptake. In conjunction with basic plant requirement, extraneous physical/chemical conditions may prohibit reserve N from being plant available, further compounding the definition of need. It has been shown that N concentration, physical, and chemical parameters exhibit spatial variability. Spatial variability, in this case, is the observable difference in growing environments continuously varying over space. As a consequence N availability and potential uptake are subject to variance in soil conditions at the process scale in which soil conditions significantly vary. Therefore, alignment

between process and measurement scale plays an important role in determining strategies for N application. Current methodology in N management should be focused, not only in mass balance, but also should incorporate spatial variability and site-specific definitions of need.

Previous research suggests that plant response to supplemental N and biomass can predict yield and a yield based N recommendation can improve N use efficiency. Chapter 2 of this study analyzes the current calculation of response index and defines a continuous response index (RI) function at the process scale. This research is focused at understanding the relationship between residual N sufficiency and sufficiency reached through N supplementation. Given reasonable stationarity in the field, examination of plant response in experimental conditions should indicate how likely the field would utilize supplemental N.

Objectives of Chapter 2:

- Clearly understand and quantify the relationship of N response to varying levels of plant stand as measured by NDVI.
- Formulate application boundaries where supplemental N is most effective as measured by RI.
- Incorporate agronomic boundary conditions in the framework of RI estimation.

Chapter 3 promotes a combination of agricultural research with the GreenSeeker™ optical sensor and remote sensing methodology (spectral mixture models) to estimate fractional vegetative cover (FVC) per experimental unit. Several experiments show that vegetative cover is correlated to the normalized difference vegetative index (NDVI), such that decreased NDVI variability implies high vegetative coverage. From a

statistical standpoint, low variance should also exist for experimental units with low (≈ 0) NDVI (bare soil). Thus, NDVI variability is a measure of plant stand homogeneity. This ideology can be used to estimate spectral endmembers for use in a spectral mixture analysis (SMA) model. Remote sensing literature shows that a linear two-endmember SMA model is often used in conjunction with NDVI images to estimate FVC. Recent agricultural literature confirms that through a combination of digital imagery and/or the GreenSeeker^{TM} sensor FVC is linearly related to NDVI. The combination of these findings should produce a method of determining vegetative cover. Accurate estimation of FVC may hold the promise of adding extra information to the yield prediction process.

Objectives of Chapter 3:

- Develop a clear spectral definition of bare soil and 100% vegetation cover.
- Formulate a methodology of estimating vegetative coverage using spectral measurements from existing optical sensor technology.
- Incorporate remote sensing methodology (spectral mixture models) with recent agricultural research.

Long study of the NDVI - yield relationship has developed theoretical models that fit with field collected data. Recent studies, however, have produced new information about a plant response to N. Chapter 4 proposes a continuous sigmoidal yield potential prediction using agronomic boundary conditions. Existing models do not estimate yield for low NDVI and uses a piece-wise exponential model to estimate yield increase until a biophysical cap is reached constraining further increase. Conceptually, yield is low for low NDVI, increases exponentially through mid-range NDVI, and plateaus for high NDVI. Given recent findings, conceptual constraints, and boundary conditions Chapter 4

further defines a continuous sigmoidal growth model to estimate yield potential (YP_0) from NDVI using continuous plant response to N and defines a sigmoidal approach to yield potential under varying N application rates incorporating continuous RI_{NDVI} (YP_N model). In concert, these models can be used to estimate gain in yield potential, which forms the basis of an economic approach to conservative N application.

Objectives of Chapter 4:

- Incorporate agronomic boundary conditions and recent findings into a continuous yield prediction model.
- Validate the consistency of a continuous yield model against empirical models.
- Develop a strategy of utilizing the continuous RI model as a method of predicting the affect of supplemental N in improving yield.
- Develop the basis of an economic method to determine financially optimal N application for variable rate technology.

The purpose of this dissertation is to develop management tools and theory that promote economically efficient N application, thereby creating positive externalities for environmental protection. Because of limited risk to human health and environmental degradation N is allocated less public concern and will not likely be managed unless human risk is verified. However, as fertilizer prices continue to rise, excessive N application presents a higher loss margin as loss in productivity. It is likely that environmental concerns about excessive N application will be addressed secondary to profit margin maximization. Nevertheless, it is likely that economically conservative management of N will produce fortuitous benefits for the environment.

Objectives of the Dissertation:

- Develop robust models for yield and fertilizer response, which conform to agronomic and spectral theory.
- Combine proposed models with existing theory to construct agronomic and economic optimal N rate application recommendations.

CHAPTER II

A CONTINUOUS FUNCTION TO PREDICT PLANT RESPONSE TO APPLIED NITROGEN

Abstract

Adequate estimation of plant response to applied nitrogen (N) is an essential step in predicting yield and increasing nitrogen use efficiency (NUE) in agronomic systems. Increasing NUE, by accurate estimation of residual N reserves, can serve as an economic and environmental net positive if set as a management goal. Previous studies show N reserves can be gauged in-field without the use of extensive soil testing by remote sensing methods through the normalized vegetative index (NDVI). The response index (RI), a measure of plant response to applied N given concentrations of residual N reserves, can be calculated as the ratio of the NDVI from N treated and non-treated plots. Current methodology assumes that RI is a field level constant disregarding process scale. This paper presents a non-linear regression methodology to predict plant response to applied N. Further, work in this paper shows that a plant response to N prediction model is possible and is robust across wheat, bermudagrass, and corn cropping systems. Additionally, the model predicts the effect of varied N application rate and confirms previous work suggesting N has little effect if applied on high residual N plant stands (i.e. NDVI > 0.73). As a result of this functional relationship, prediction of plant response to applied N (RI) is improved.

Introduction

It has long been realized that Nitrogen (N) application, when not fully utilized in-field, results in environmental degradation and financial loss. The National Research Council executive study in precision agriculture succinctly makes the point that "agricultural pollution comes from inputs that do not reach their target…" and "…inputs that contribute to pollution are thus wasted from a productivity point of view" (NRC 1997: p85). These statements outline the two basic interrelated problems in profitable industrialized agriculture –social cost through environmental degradation and profitability loss through lost opportunity and wasted inputs.

Recently, it has been a goal of precision agricultural research to decrease the amount of wasted N through site-specific management and variable rate application addressing spatial and temporal scales. While estimates of N waste vary, Johnson and Raun (2003) show that N use efficiency (NUE), the amount of applied N recovered in cereal grain, is on average less than 33% globally. In the typical case, the remaining 67% N not recovered in product either is bound in the plant/soil matrix or is, more likely, transported off-site by various modes of N migration. Current research shows that a 20% increase in NUE could result in a near $11 billion savings world-wide (NUE, 2008). Implicitly, cost savings will likely become larger as petroleum based fertilizers increase in price. Recently the USDA reported that the cost to the farmer for ammonia-based fertilizer (Ammonium Nitrate) has increased 130% between 2000 and 2006 (Huang, 2007) with demonstrable potential for further increase. Fortunately, methods of reducing N waste to improve economic efficiency, by cutting costs, also creates a positive externality of reducing environmental damage.

The Environmental Protection Agency (EPA) contends that excess N in water supplies is linked with human health problems, such as methemoglobinemia (Blue Baby Syndrome) and non-Hodgkin's Lymphoma. Further, N liberated into the atmosphere may also contribute to quality of life issues, such as ozone indulgence increasing the number of ozone alert days directly affecting persons with respiratory problems. Additionally, excess N in surface runoff contributes to general surface water supply degradation, such as increased eutrophication (EPA1 2007) and aquatic fauna mortality (Hecnar 1995; Hatch et al. 2001). Other researchers have linked N loadings to accelerated eutrophication and hypoxic conditions in larger waterways such as the "Dead Zone" at the mouth of the Mississippi River (Turner and Rabalais, 1994; Rabalais et al., 1996; NOAA 2007). Increased hypoxic conditions can have severe social economic implications for estuarial aquaculture and the dependent communities. It is clear that, while exact social cost through degradation may not be fully realized, there is a potential for both human health and environmental issues on the horizon from excess N.

Nitrogen application to areas of low plant N uptake increases plant-soil system reserve N and increases the potential for off-site migration. To lower off-site migration potential, it is necessary to identify conditions contributing to low uptake and adjust N application accordingly overall increasing NUE. Raun et al. (2005a) suggests that N application based on a combination of predicted yield and plant response to N can increase NUE by 15% over standard application practices, which verified earlier work by Johnson and Raun (2003) advocating the inclusion of plant response to N as a critical component in increasing NUE. In general, NUE is decreased by supplementation above sufficient N levels, which can be recognized by low responsiveness.

Work by Johnson et al. (2000) proposed a response index ($RI_{Harvest}$) to represent the plant response to supplemental N, which was based on the proportion of yield between N treated and non-treated plots.

$$RI_{Harvest} = \frac{Yld_{NRich}}{Yld_{FieldRate}} \tag{2.1}$$

where Yld_{NRich} is the average yield within a Nitrogen rich strip and $Yld_{FieldRate}$ is the average yield in an adjacent non-fertilized strip. This estimate, however accurate, is based on post-season measurements and fails to address in-season N application. Earlier findings by Stone et al. (1996) showed that plant biomass could be measured by using optical sensor measurements of light reflection. Mullen et al. (2003) later proposed the use of an in-season response index (RI_{NDVI}) based on a ratio of the normalized difference vegetative index (NDVI) between treated ($NDVI_{NRich}$) and non-treated ($NDVI_{FieldRate}$) plots that reasonably correlated ($r^2 > 0.56$) with post-season response ($RI_{Harvest}$).

$$RI_{NDVI} = \frac{NDVI_{NRich}}{NDVI_{FieldRate}} \tag{2.2}$$

Raun et al. (2005a) demonstrated that while RI_{NDVI} tends to underestimate $RI_{Harvest}$, it serves as a conservative estimate of yield increase with N supplementation. They further proposed a methodology to calculate N fertilizer application rates from NDVI measurements. They enumerated three fundamental postulates necessary to calculate N rates: 1. Yield potential could be predicted accurately midway through the growing season with an exponential model of yield as a function of NDVI. 2. The response to additional N fertilizer is a constant multiple of the yield potential. 3. There exists a maximum yield for any location that is a function of all the agronomic and environmental factors for that location, and yield cannot exceed that limit for any N fertilizer rate of

additional fertilizer (Fig. 2.1). Nitrogen fertilizer rate was a function of the difference between the yields with and without additional fertilizer multiplied by the percentage of N contained in the grain divided by the efficiency by which the plant absorbed applied N for grain production (Nitrogen Use Efficiency).

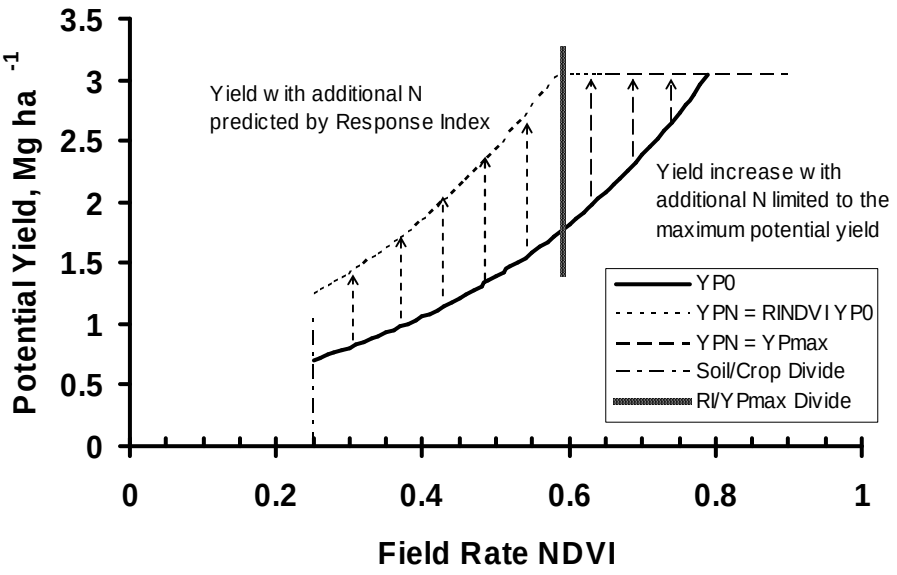

Figure 2.1. Change in Potential Yield of Wheat with Additional N Fertilizer for a Response Index of RI = 1.5, a Maximum Potential Yield of 3.0 Mg Ha^{-1} and 120 Days After Planting (Raun et. al, 2005a).

Under this methodology yield potential is exponentially related to field rate NDVI given by:

$$YP_N = a(RI_{NDVI})e^{b(NDVI)} \text{ for : } YP_N < YP_{Max}; RI_{NDVI} = 1 \text{ for } N = 0 \qquad (2.3)$$

where yield potential (YP_N) is a function of field rate NDVI and plant response due to N application rate (RI_{NDVI}) ranging between 0 kg N ha^{-1} N and sufficient concentrations. Obviously, 0-N application results in no complementary plant response (RI=1); however, RI is allowed to increase proportionate to increases in N application rate, which increases the overall function. Overall yield increase is constrained under a constant biological

yield maximum obtainable from the field (YP_{max}). As a result, N supplementation drives the relationship to YP_{Max} quicker, in terms of field rate NDVI where RI_{NDVI} acts as a multiplier. RI_{NDVI} based on yield potential can be defined as:

$$RI_{NDVI} = \begin{cases} \dfrac{YP_N}{YP_0} & \text{for } YP_N < YP_{Max} \text{ and NDVI} > 0.25 \\ \dfrac{YP_{Max}}{YP_0} & \text{for } YP_N \geq YP_{Max} \text{ and NDVI} \leq 0.73 \\ 1 & \text{for } YP_0 \rightarrow YP_{Max} \text{ and NDVI} > 0.73 \end{cases} \quad (2.4)$$

This definition of RI_{NDVI} combines the Johnson et al. (2000) $RI_{Harvest}$ and Mullen et al. (2003) RI_{NDVI} under yield potential. Specifically, for this piecewise definition, RI_{NDVI} is a constant and is independent of non-fertilizer NDVI until YP_{Max} $(NDVI \approx 0.57)$ is reached, after which it becomes inversely proportional to non-fertilizer NDVI until a biological maximum is reached at $(NDVI \approx 0.73)$. Additionally, meaningful yield potential is restricted to field rate NDVI values greater than 0.25, which represents the soil-crop divide and was derived by field observation (Raun et al. 2005a). Overall, the method by which RI_{NDVI} is calculated relies on a ratio of average NDVI for treated and non-treated areas at the plot level, which neglects measurement scale effect.

Solie et al. (1996) addressed the issue of measurement scale effect and advocated working at a fundamental field element where nutrient concentrations vary as a function of distance and were detectable. Taylor et al. (1999) found that variation in yield decreased as plot size decreased, indicating a proportional relationship between variance and scale. These studies indicate a process scale exists at which variation should be

treated to optimize nutrient management. Raun et al. (1998) found that significant differences exist between soil tests at less than 1m separation distance. Solie et al. (1999), using geostatistical methods, showed that the semivariogram range varied from 1.04m to 6.70m, variable dependent, and that the integral scale (zone of high relatedness) was at the sub-meter to meter level. These studies suggest a process scale at or below 1m and argue for adopting a commensurate measurement scale to accurately treat spatial variation. Treatment of spatial variation at the process scale mitigates the effects of bias of small-scale variation aliased into larger variation (Journel and Huijbregts 1978; Russo and Jury 1987; and Western and Bloschl 1999).

Fundamental work by Johnson et al. (2000) developed a measure to quantify the relationship between residual N and response due to N supplementation ($RI_{Harvest}$) post-season, which led to the concept that plant response to additional N is dependent on sufficiency of residual N in the plant-soil matrix (Johnson and Raun, 2003). Consequent to these findings, Mullen et al. (2003) proposed a methodology to calculate RI values directly from NDVI measurements (RI_{NDVI}) that worked mid-season. Raun et al. (2005a) revised RI_{NDVI} as a combination of previous RI calculations, which is used in predicting yield potential mid-season. This method, however, uses a plot averaged RI_{NDVI} as a constant to adjust yield for overall plant response to N supplementation, and implies that RI_{NDVI} is constant until YP_{Max} $(NDVI \approx 0.57)$ is reached, variable until a biological limit is reached $(0.57 \leq NDVI \leq 0.73)$, and constant at RI_{NDVI} =1 after a biological limit is reached (NDVI > 0.73).

The purpose of this study is to quantitatively determine the relationship between RI_{NDVI} and non-fertilizer NDVI by method of paired comparison at finer (1m < experimental unit < 4m) than plot scale resolution.

Methods and Materials

Data in this study represent five years (2002 – 2006) of collections on 19 sites in north-central Oklahoma producing 6,356 sample pairs across three species (bermudagrass, wheat, and corn). Each sample pair consists of the normalized difference vegetative index (NDVI) for an N treated sample (SpNDVI) and a nearest neighbor non-treated sample (FpNDVI). Here FpNDVI represents the farmer practice or initial condition NDVI prior to N supplementation. It is implied that FpNDVI is a measurement of plant stand health relying on previous nutrient reserves. Subsequently, SpNDVI is a spectral measure of plant stand health based on existing soil nutrients plus supplemental N from fertilizer at an application rate great enough to remove N as a yield limiting factor.

A response index (RI) value was calculated for each experimental pair, using the Mullen et al. (2003) expression for RI_{NDVI} calculated from mid-season measurements of NDVI where:

$$RI_{NDVI} = \frac{SpNDVI}{FpNDVI} \tag{2.5}$$

RI_{NDVI} is a normalized estimate of plant response to supplemental N above previous practice and is related to the increase in plant biomasss. For computational purposes NDVI values were constrained between [0, 1] where negative NDVI values were set to 0 constraining RI_{NDVI} between $[0, \infty)$. Since NDVI is a function of biological and physical

factors, indeterminate conditions where SpNDVI = FpNDVI = 0, RI was set to 1 by extension of L'Hopital's Rule (Finney et al. 1994).

All N treated experimental units received post planting topdress Urea-Ammonium Nitrate, UAN (solution 28% or 32%), while corresponding check plots did not receive supplemental N. Treatment design and N level were varied over the 19 sites. Five sites were sampled by calibration stamp design (Raun et al. 2004), which is a 3m x 3m matrix of 9 – $1m^2$ plots, consisting of four check plots and five incremental treatment plots. Application rates were 22, 45, 67, 90, and 112 kg N ha^{-1} (20, 40, 60, 80, and 100 lbs N $acre^{-1}$) and were placed in wheat and bermudagrass in 2004. Each calibration stamp was sensed at $1m^2$ resolution with the hand-held Greenseeker™ optical sensor (Ntech Industries, Ukiah CA.). The plots were sampled four times at intervals of two weeks after N application and averaged together. Thirteen sites contained an N-rich strip (Solie et al. 2002) design in which a top-dress nitrogen (112 kg N ha^{-1}) transect was applied across an operative farm field, in wheat only. Nitrogen rates were expected to be high enough so that N was a non-limiting nutrient. Of the 13 sites, four fields were sampled in 2003 at 0.81m - 1.2m resolution using a field scale GreenSeeker™ sensor/applicator array described in Solie et al. (2002), while the remaining nine sites were sampled during the growing seasons of 2002 and 2003 using IKONOS (Space Imaging LLC, 12076, Thorton, CO. 80241*)* 4m resolution satellite imagery. The IKONOS imagery was geographically processed to identify nearest-neighbor sample pairs. The early-season topdress UAN strip appeared in subsequent satellite imagery as a band of high NDVI pixels, which was selected and paired by image processing software to adjacent nearest spatial neighbor pixels not in the strip using a geographical first order search algorithm.

The last observation site is composed of average corn responses from twelve sites collected during 2002 – 2004 growing seasons (Teal et al. 2006 and Freeman et al. 2007). Experimental corn plots were arranged by randomized complete block design and varied in size (3.0 x 6.1m and 3.0 x 9.1m). Linking averaged treatment plot NDVI to adjacent check plot NDVI created the sample pairs used in this dataset.

Once these data were compiled, it was necessary to filter unrealistic values. The IKONOS dataset, due to spatial alignment, contained a minority of FpNDVI points at or close to zero paired with substantially higher SpNDVI points that resulted in extreme RI_{NDVI} values. Specifically, large (4m) resolution compounded by misalignment between transect and image occasionally resulted in nearest neighbors greater than 12m apart. These dispersed neighbors had little spatial relationship, which when ratioed produced improbable RI values. Solie et al. (1999) showed that distance dependence ranged between 1.04m and 6.70m for most soil test variables, which explains the value disconnect. Therefore, a two-stage filter was designed to selectively remove RI values 3.5 standard deviations from the mean sum and difference of SpNDVI and FpNDVI, respectively. Data were filtered if above or below:

$$\text{Mean}_{(\text{SpNDVI}\pm\text{FpNDVI})} \pm 3.5\text{S}_{(\text{SpNDVI}\pm\text{FpNDVI})} \quad (2.6)$$

The majority of pairs that were removed coincided with large (>12m) separation distances and all were from IKONOS imagery.

Results

Analysis of the composite dataset shows that the relationship of plant response (RI_{NDVI}) is non-linear and inversely proportional to FpNDVI. Figure 2.2 shows filtered FpNDVI plotted against RI for treatment at 112kg N Ha^{-1}.

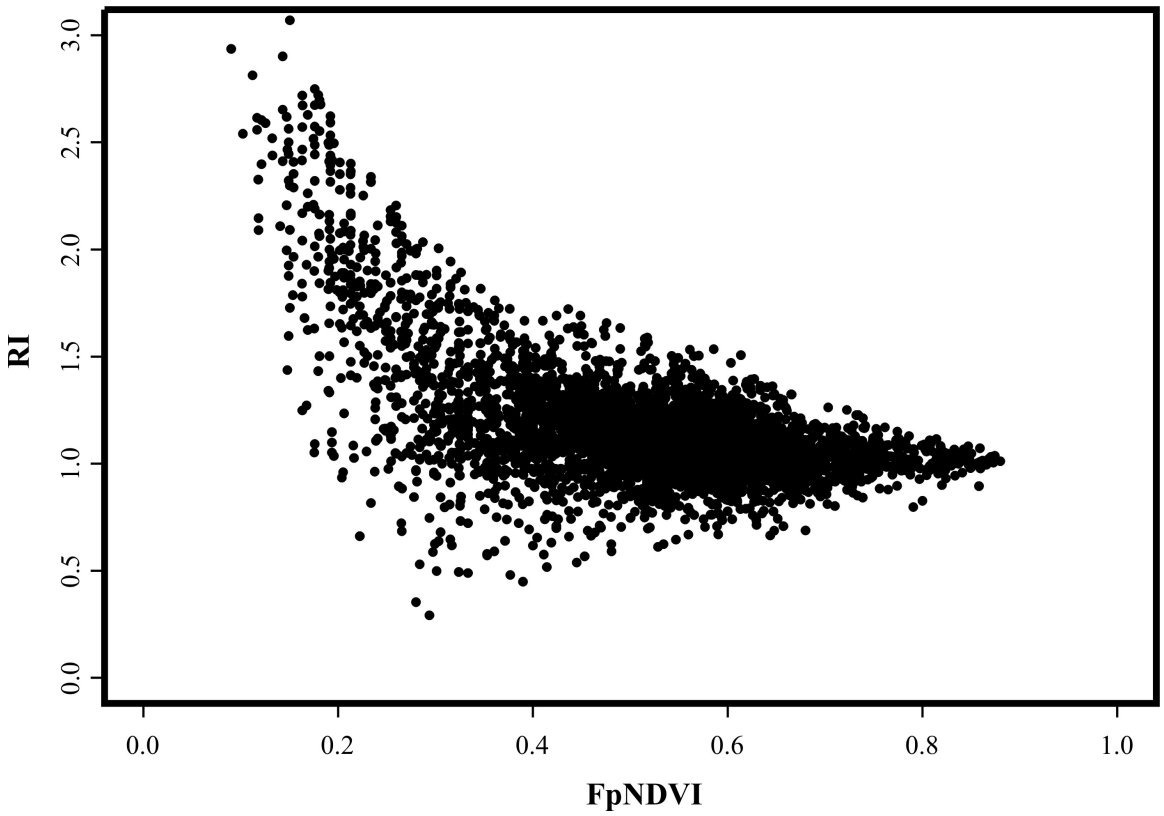

Figure 2.2: Farmer Practice NDVI (FpNDVI) Versus Response Index (RI_{NDVI}) for All Species and Locations Filtered for Extreme Data.

Data in Figure 2.2 identify an increasing independence between N treatment and plant response as FpNDVI increases. In general, plant response to N supplementation (RI_{NDVI}) is less in healthy plants (high FpNDVI) than in areas of limited growth or erratic stands (low FpNDVI). In healthy plant stands, near the biological maximum growth, where residual N is sufficient, additional N shows little effect on crop growth as evidenced by low values of RI_{NDVI}. Conversely, increased plant response for lower FpNDVI demonstrates N limited conditions where supplementation produces high RI_{NDVI}. However, because the response index is proportionate to N supplementation and the denominator (FpNDVI) is small, poor stands, regardless of real increase in biomass, will demonstrate a nominally high N response. Additionally, crops with low FpNDVI exhibit

considerable scatter, with some values falling below $RI_{NDVI} = 1$ while other sample pairs exceed $RI_{NDVI} = 3$. This is likely due to a range of physical and chemical phenomena existing in the field. However, there is some amount of certainty that responses with $RI_{NDVI} \to 1$ (no response) indicate plant stands where N is a minor factor limiting treatment response.

Quantification of the inverse exponential relationship of RI_{NDVI} to FpNDVI requires a non-linear regression model that expresses a maximum response and allows RI to decrease at a decreasing rate until becoming asymptotically independent from supplemental N. Additionally, it is necessary to enforce boundary conditions such that FpNDVI = 0 implies $RI_{NDVI} = 1$. Given that FpNDVI = 0 implies bare soil, supplemental N should have no effect (SpNDVI = 0). Assuming the FpNDVI and SpNDVI are spectral functions, L'Hopital's Rule guarantees a value for RI_{NDVI} for the indeterminate condition $RI_{NDVI} \to 1$.

The proposed model for predicting RI_{NDVI} is a peak function with regression parameters controlling maximum response and exponential decrease. Several models were evaluated on the criteria of minimizing the residual sum of squares (RSS) with the fewest control parameters. The coefficient of determination was not used in model selection because it cannot be insured that the sum of squares error plus the sum of squares from regression equal the total sum of squares (Neter et al. 1996). The best of these models, by minimization of RSS, was a two-parameter inverse hyperbolic cosine

$$RI_{NDVI} = \frac{A_0(\text{FpNDVI})}{\cosh(A_1 \text{FpNDVI})} + 1 \qquad (2.7)$$

where A_0 and A_1 are regression parameters derived through a non-linear least squares estimation (Gauss – Newton Method). Parameter A_0 controls maximum response while parameter A_1 controls the rate of decrease from maximum response to the asymptote. Figure 2.3 shows the visual fit of the model to these data.

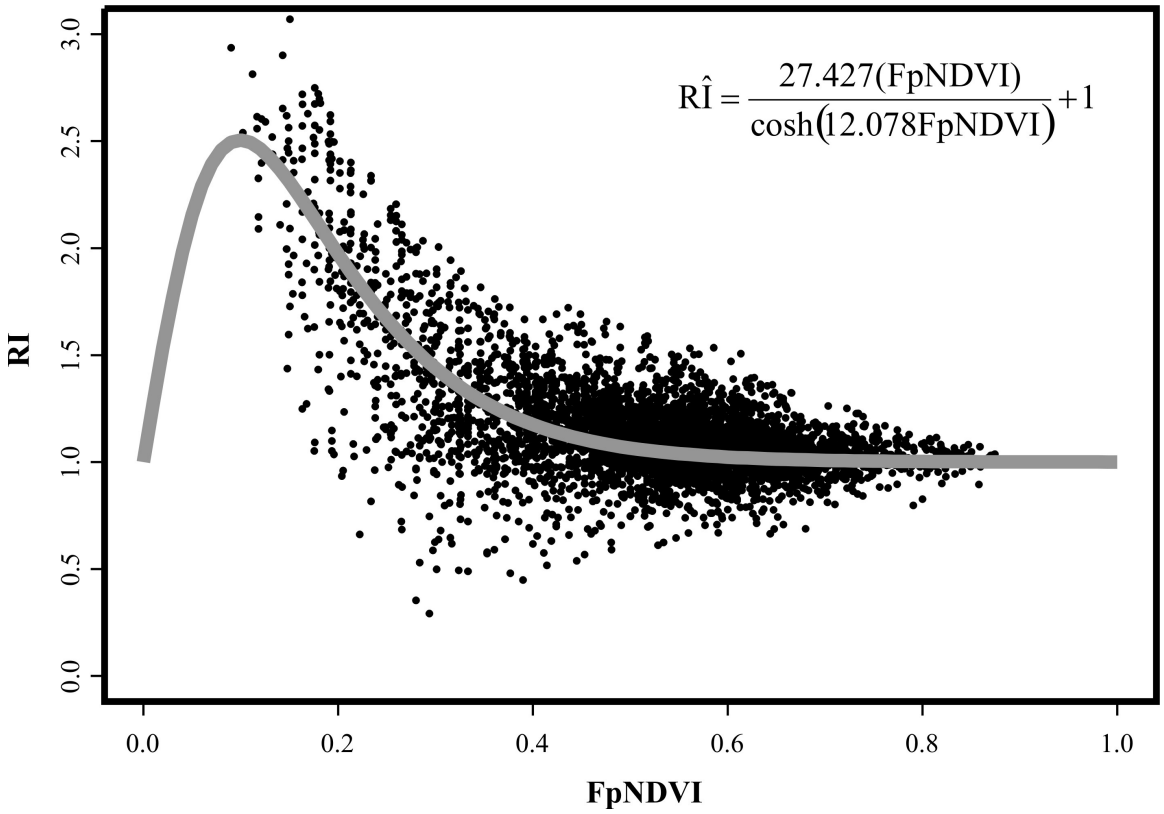

Figure 2.3: Hyperbolic Cosine Regression Model of RI_{NDVI} as a Function Farmer Practice NDVI.

Results of the fit are visually acceptable (Figure 3) with the trend line passing through the center of the data distribution. The function maximum shows that RI_{NDVI} is most likely to reach a maximum for low values of FpNDVI. Maximum response occurred in areas where the plant stand was erratic or crop growth was greatly reduced compared with spatially related areas with sufficient N. In these areas of sparse plant stands, even minimal increase in SpNDVI due to supplemental N is, by proportion, very large. Raun et al. (2005a) concluded that the magnitude of the agronomic and economic benefits from

supplemental N were so small that N fertilizer should not be applied in regions where FpNDVI<0.25.

The slope of the exponential curve declines from the maximum response to the RI_{NDVI}=1 asymptote as FpNDVI increases, defining the sensitivity of plant response to supplemental N per incremental increase in FpNDVI, after maximum response has been achieved. Generally, a steeper transition slope indicates N sufficiency is reached at lower values of FpNDVI demonstrating that N is no longer the primary limiting factor. Shallower transition slopes indicate that additional N strongly influences crop response until independence is reached. Plants near biological maximum growth, high FpNDVI, are N sufficient and independent of supplemental N.

The basic equation (Equation 2.7) to derive the model in Figure 2.3 assumes that the spectral definition of bare soil is FpNDVI = 0. However, many cases in this research show that the FpNDVI definition of bare soil (Ns) may range 0 < FpNDVI < 0.15. To correct this issue Figure 2.4 demonstrates a translation adjustment for the RI_{NDVI} curve.

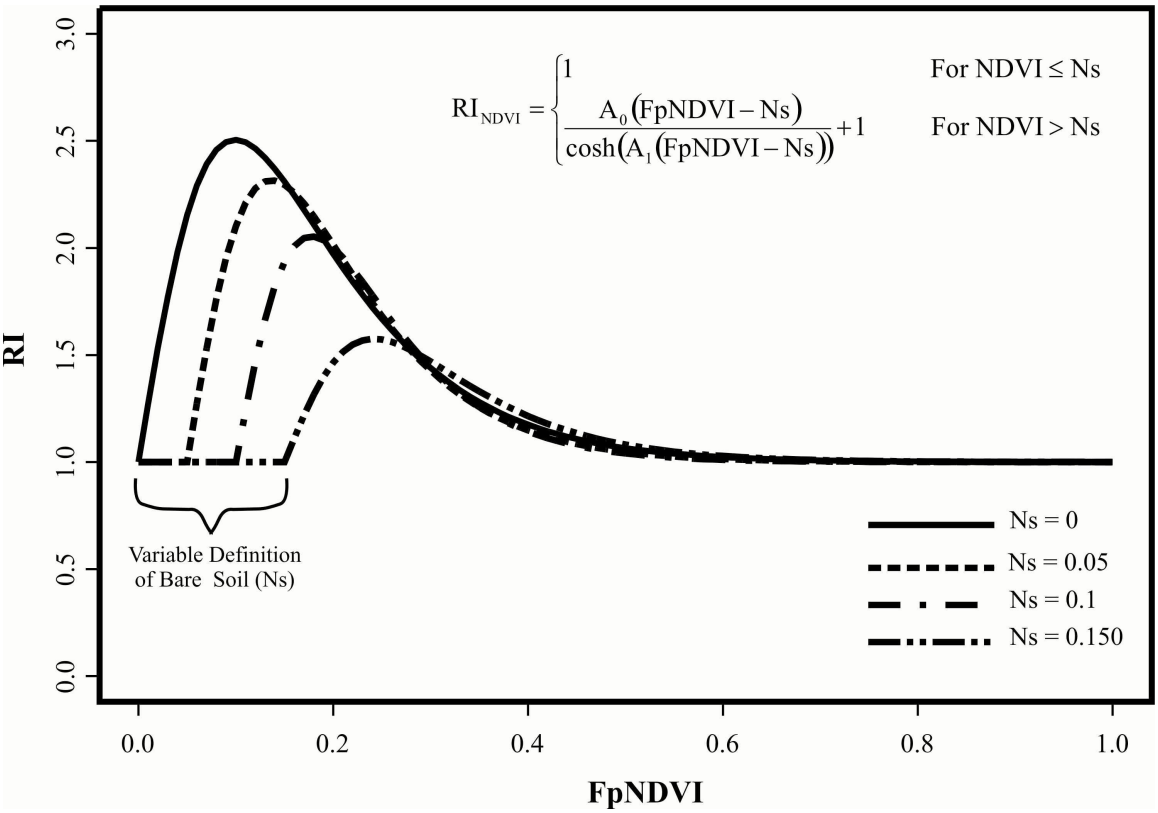

Figure 2.4: The Effect The Variable Bare Soil NDVI (Ns) Definition on the Response Index Curve, where Bare Soil Ranges 0 < NDVI < 0.150.

Figure 2.4 shows that as Ns increases the magnitude of maximum response decreases proportionately. Additionally, for RI_{NDVI} to be continuous across the FpNDVI spectrum it is necessary to define $RI_{NDVI} = 1$ for $0 \le \text{FpNDVI} \le \text{Ns}$, and RI_{NDVI} equal to the hyperbolic cosine model for FpNDVI > Ns. Equation 2.8 describes the bare soil (Ns) offset in a piece-wise model

$$RI_{NDVI} = \begin{cases} 1 & \text{For NDVI} \le \text{Ns} \\ \frac{A_0(\text{FpNDVI} - \text{Ns})}{\cosh(A_1(\text{FpNDVI} - \text{Ns}))} + 1 & \text{For NDVI} > \text{Ns} \end{cases} \quad (2.8)$$

In the general case where Ns = 0 the function reduces to Equation 2.7, which is useful for comparing curves in different plots where the NDVI of bare soil was not collected.

Across species, consistency of the model and the robustness of the relationship were classified by species receiving 112kg N Ha^{-1} (Fig. 2.5).

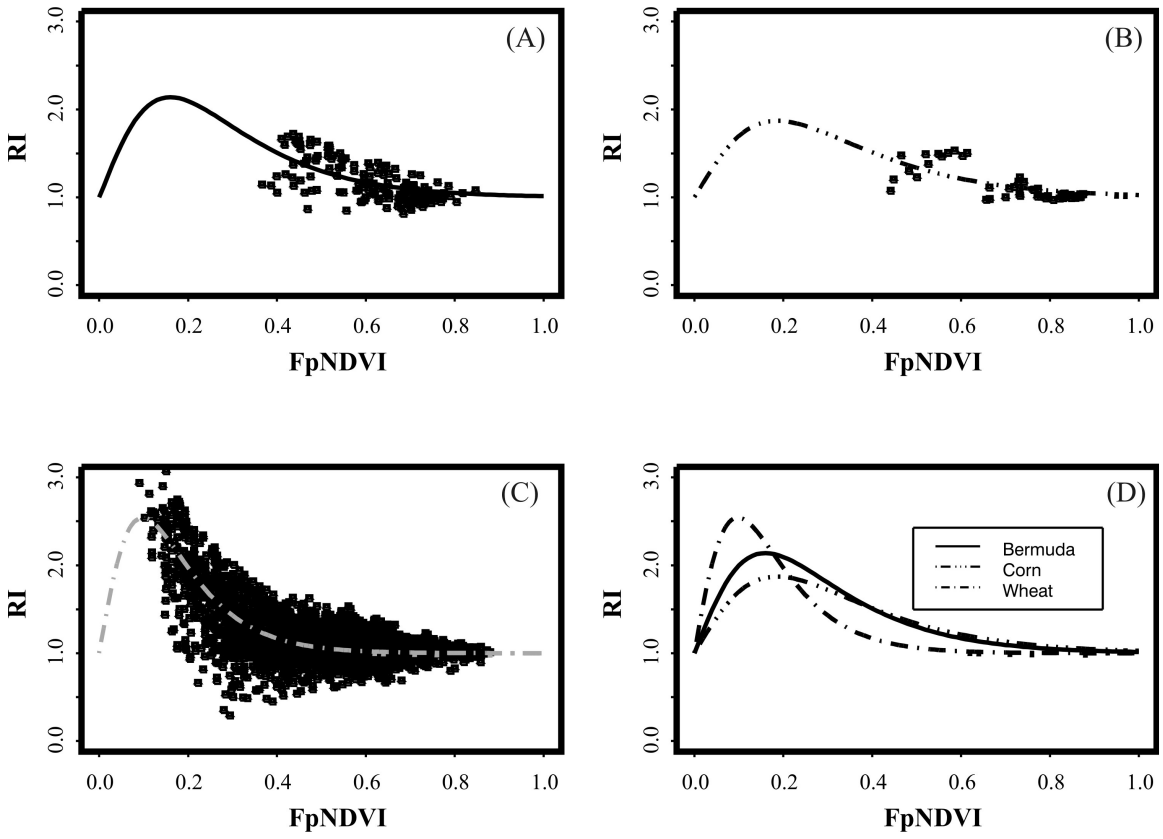

Figure 2.5: Model Fit by Species for RI_{NDVI} as a Function of Farmer Practice NDVI Assuming Ns = 0. Parameter for species A: Bermudagrass (A_0 =12.940, A_1= 7.528), B: Corn (A_0 =8.474, A_1= 6.449) and C: Wheat (A_0 =28.604, A_1= 12.297), and D: Relative Comparison of Curves.

Figures 2.5 (A, B, and C) show that the same asymptotic response trend exists across species as $FpNDVI \rightarrow 1$. Bermudagrass (Figure 2.5A) and corn (Figure 2.5B) experiments tend to be clustered at higher FpNDVI values because data were collected from a limited number of locations and these sites were experimentally controlled plots with a higher degree of environmental consistency and low plot variability whereas there was a large number of wheat (Figure 2.5C) trials, which occurred both in controlled plots and in farm fields and over several years.

To assess different treatment levels, the model was reparameterized for each applied N rate: 22, 45, 67, 90, 112 kg N Ha^{-1} (Figure 2.6).

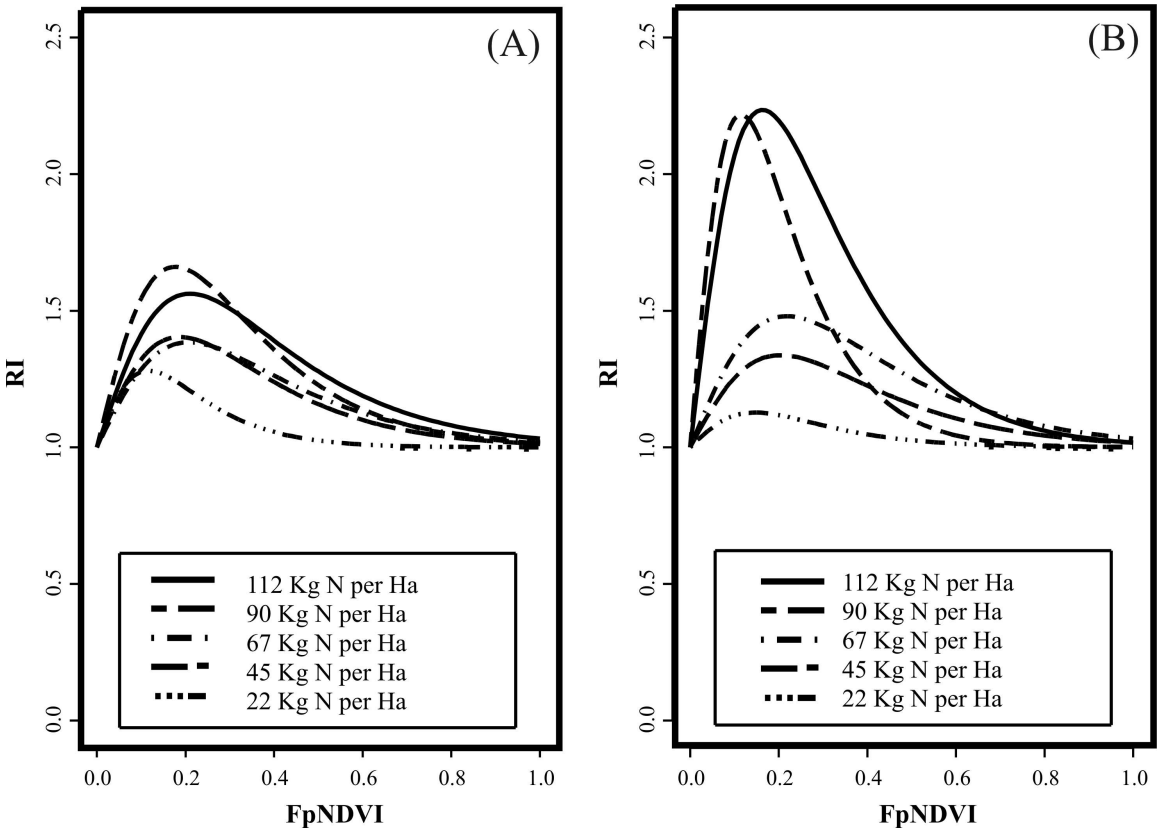

Figure 2.6: N Fertilizer Treatment Level Response Curves for RI_{NDVI} in Wheat (A) and Bermudagrass (B) Under Calibration Stamp Design Assuming Ns =0.

Maximum response in wheat (Figure 2.6A) is much lower, overall, than bermudagrass (Figure 2.6B) collected under the same design structure. Wheat sampled in the calibration stamp design was grown in experimental plots which received regulated N treatment in the previous growing season; bermudagrass, however, did not have N applied in the previous year. This indicates that maximum response is highly dependent on residual N from previous treatments and/or pre-plant conditions. Table 2.1 shows the modeling parameter shifts.

Table 2.1: N Application Rate RI_{NDVI} Parameter Values

N Rate (kg N ha^{-1})	A_0	A_1
112	4.84	5.71
90	6.76	6.78
67	3.36	5.78
45	3.91	6.41
22	4.37	10.33

Table 2.1: N Application Rate in kg ha^{-1} Influenced Parameter Shifts.

Regardless of previous management, it appears that limited N application inhibits maximum response. Response to supplemental N is sensitive to application rate, in addition to N available from non-application sources. In fact, wheat may be sensitive, at least at low NDVI, to over application. Figure 2.6A shows that 112 kg N Ha^{-1} has a lower maximum response than 90 kg N Ha^{-1} application rate. In comparison, bermudagrass (Figure 2.6B) exhibits strong response to N supplementation at lower values of FpNDVI, but transitions to N sufficiency quickly, whereas wheat, with a lower maximum response, transitions at a much slower rate. This indicates that bermudagrass in this experiment had limited available N causing lower FpNDVI values, but transitioned into sufficiency very quickly due to limitations from other physical/chemical sources, primarily Phosphorus (Table 2.2). Wheat had a higher non-fertilizer NO_3 concentration at low FpNDVI and supplemental N remains a primary factor in response (Table 2.2).

Table 2.2: Average soil pH, NO_3, STP, K, and EC values for Wheat and Bermudagrass Plots.

Species	pH	NO_3 ($kgha^{-1}$)	STP ($kgha^{-1}$)	K ($kgha^{-1}$)	EC (mmhos/cm)
Wheat	5.9	5	30	266	102
Bermudagrass	5.7	2	17	173	39

Table 2.2: pH, NO_3 = Nitrate, STP = Soil Test Phosphorus, K = Potassium, EC = Electrical Conductivity Measured by Soluble Salt Content.

Figure 2.6 (A and B) show that RI_{NDVI} curves at high FpNDVI converge to RI_{NDVI} = 1. Wheat, at the maximum application rate, declines to 10% response above no N rate (RI_{NDVI} =1.1) at FpNDVI ≈ 0.75 and bermudagrass at FpNDVI $\approx$ 0.73. At this level, the five application rates are relatively indistinguishable from each other (wheat =3.65% and bermudagrass = 4.25% difference in response across application rates). Values greater than FpNDVI = 0.75 RI_{NDVI} continue to converge, and the difference between application rate curves becomes indistinguishable as $RI_{NDVI} \rightarrow 1.0$.

Discussion

This experiment examined the relationship between RI and farmer practice NDVI using paired comparisons at or near the fundamental field element size suggested in Raun et al. (1998) and Solie et al. (1999) and found that RI_{NDVI} is highly related to residual N as measured by NDVI (FpNDVI) at the (< 4m) sensing level. These data show a characteristic exponential decline in RI_{NDVI} as FpNDVI increases, which suggest an increasing independence between supplemental N and response. Generally, areas of low NDVI, or low biomass, exhibited high sensitivity to N supplementation because N was likely the dominant limiting factor. As biomass increases, indicated by increasing higher NDVI, residual N is more available, and these areas are less responsive to supplemental N. Ultimately, at high levels of biomass, high NDVI, residual N nears sufficiency, and N supplementation produces little to no plant response.

A non-linear peak function was developed to quantify the relationship dictated by the dataset. It was necessary to use a peak function because of imposed boundary conditions. Conceptually, for extremely low NDVI, at or near bare soil, N supplementation should not cause a response in NDVI. Similarly, N supplementation at

high NDVI, high biomass, should not result in response due to residual N sufficiency. While boundary conditions were established previous to the model, these data, by non-linear regression techniques, were used to estimate the peak (maximum response) and the rate of decline (transition rate), the parameters for which are A_0 and A_1, respectively (Equation 2.7). Additionally, since the hyperbolic peak function assumes FpNDVI = 0 for bare soil, it was necessary to account for alternate NDVI definitions of bare soil. This was accomplished by adding a bare soil NDVI translation parameter (Ns) to the hyperbolic peak model and specifying $RI_{NDVI} = 1$ for $0 \leq$ FpNDVI $\leq$ Ns (Equation 2.8). There is constant (slope = 0) no response ($RI_{NDVI} = 1$) for bare soil completely devoid of plant material. However, for a single instance of plant material RI_{NDVI} can increase with a variable slope potential described by the inverse hyperbolic cosine model.

It should be noted that this study used an amalgamation of different datasets sampled at various growth stages of those respective plant stands. It has been shown that spectral indices (NDVI), plant response to supplemental N, and stand variability are sensitive to growth stage (Sembiring et al. 2000 and Raun et al. 2005b). Growth stage, time from planting to sensing, and time from fertilization to sensing were not considered in this research. Specifically, Figures 2.2 and 2.3, by aggregation of data, represent a multiple field average response without consideration of growth stage and it is acknowledged that growth stage can alter the response model, specifically magnitude of maximum response. Further research should be conducted to better understand the temporal aspects of response.

It was necessary that the model be consistent across species (crops) for it to be useful as an agronomic tool. The overall connection between RI and NDVI appears to be

standard across species, in that only parameter differences were detectable across bermudagrass, corn, and wheat. Bermudagrass tended to have higher maximum response and a steeper transition; this is likely because bermudagrass calibration stamps were on locations with limited fertilizer management and tended to be compositely nutrient limited. Wheat calibration stamps were placed in previously managed locations, had higher residual N concentrations, and were shown to be less nutrient limited. High maximum response at low NDVI concurrent with steep transition slope shows that N is limiting for low NDVI but meets sufficiency quickly as limited by other minimum resources.

In conjunction with residual N, maximum response is proportionate to supplemental N application rate. In general, as application rate decreases, maximum response decreases. Notably, maximum response decreases as a result of decreased N application rate; the transition slope is gentler and constant, which indicates that supplemental N remains a primary factor in response limitation further across the range of NDVI. Conversely, higher maximum response and steeper transition slope indicates that supplemental N, while being a primary factor for increasing NDVI, quickly transitions to a lesser role in response as NDVI increases.

The paired comparison methodology and fine resolution shows RI can be defined for NDVI <0.25 as opposed to the Raun et al. (2005a) yield potential model. This research also shows RI_{NDVI} to be variable across the entire spectrum of NDVI whereas the yield potential model implies a constant relationship until YP_{Max} is reached. Both models agree that RI_{NDVI} exponentially decreases as NDVI increases although in different ranges. Interestingly, Raun et al. (2005a) remarked that NDVI $\approx$ 0.73 represented an

upper threshold where further N supplementation would not increase yield. This experiment shows that NDVI $\approx$ 0.73 only produced 10% growth, as measured by NDVI, better than no-response and that variable rate curves are within 5% of each other. In short, the model predicts a 10% increase in RI if an optimum N application rate is used and that there is at most a 5% difference in RI between individual application rates. Hodgen et al. (2005) referred to RI < 1.10 as non-responsive where the farmer would not observe significant return from fertilizer expenditures. These findings confirm that little response is gained, regardless of N application, at high NDVI values (particularly NDVI > 0.73). Further research should focus on marginal returns for application at high NDVI.

The findings in this research in conjunction with previous research suggests that supplemental N should be applied conservatively to extremes in the NDVI spectrum, specifically for FpNDVI less than maximum response (0 < FpNDVI < Max Response) and for extremely high FpNDVI (FpNDVI >0.73). This research also suggests that supplemental N be applied proportionately to RI_{NDVI} between maximum response and sufficiency (FpNDVI $\approx$0.73). However, these application intervals are not adjusted to yield return and fertilizer cost and cannot, therefore, be used as economic guidelines. Further research should be conducted to specify particular application intervals based on net returns.

Conclusions

Findings from this research show that plant response to N supplementation is continuous and predictable at the sub-plot level and across species. This relationship is quantifiable using an inverse hyperbolic model. Specifically, this work shows that plant response is maximized for low FpNDVI because N is the primary limiting factor. For

increasingly higher FpNDVI, N becomes less of a limiting factor and plant response to supplemental N decreases. Further, plant response tends to be sensitive to N application rate, especially in low FpNDVI where N is the limiting factor. A comparison of RI_{NDVI} curves from varied N application rates show plant response becomes negligible at FpNDVI > 0.73 regardless of application rate.

References

EPA1. 2007. Environmental Protection Agency. Mid-Atlantic Integrated Assessment: Nitrogen. Accessed 3/13/2007. Available at: http://www.epa.gov/maia/html/nitrogen.html

Finney R., G. Thomas, F. Demana, and B. Waits. 1994. Calculus: Graphical, Numerical, Algebraic. Addision-Wesley Publishing: New York.

Freeman, K.W., K. Grima, D. Arnall, R. Mullen, K. Martin, R. Teal, and W. Raun. 2007. By-plant prediction of corn forge biomass and nitrogen uptake at various growth stages using remote sensing and plant height. Agronomy Journal. 99:530-536.

Hatch, A.C., L.K. Belden, E. Scheessele, and A. R. Blaustein. 2001. Juvenile amphibians do not avoid potentially lethal levels of urea on soil substrate. Environmental Toxicology and Chemistry. No. 10. 20:2328-2335.

Hecnar, S.J. 1995. Acute and chronic toxicity of ammonium nitrate fertilizer to amphibians from southern Ontario. Environmental Toxicology and Chemistry. No. 12. 14:2131-2137.

Hodgen, P. J. , W. R. Raun, G. V. Johnson, R. K. Teal, K. W. Freeman, K. B. Brixey, K. L. Martin, J. B. Solie, and M. L. Stone. 2005. Relationship between response indices measured in-season and at harvest in winter wheat. Journal of Plant Nutrition, 28: 221–235.

Huang, W. 2007. Impact of rising natural gas prices on U.S. ammonia supply. Economic Research Service USDA. Report: WRS-0702. Available at: http://www.ers.usda.gov/publications/wrs0702

Johnson, G.V., W.R. Raun, and R.W. Mullen. 2000. Nitrogen use efficiency as influenced by crop response index. p.291. Agronomy Abstracts. ASA, CSSA, and SSSA. Madison, WI.

Johnson G.V., W.R. Raun. 2003. Nitrogen response index as a guide to fertilizer management. Journal of Plant Nutrition. Vol. 26. No. 2:249-262

Journel, A.G., and C.J. Huijbregts. 1978. Mining geostatistics. Academic Press, London.

Mullen R. W., K.W. Freeman, W. R. Raun, G. V. Johnson, M. L. Stone and J. B. Solie. (2003). Identifying an in-season response index and the potential to increase wheat yield with nitrogen. Agronomy Journal. 95:347-351

Neter, J., Kutner, M.H., Nachtsheim, C.J., and W. Wasserman. 1996. Applied Linear Regression Models. 3rd ed. Irwin Publishing - Chicago.

NOAA. 2000. TOPIC 2. Ecological and economic consequences of hypoxia. Accessed 3/13/2007. Available at: http://oceanservice.noaa.gov/products/pubs_hypox.html#Topic2

NRC. 1997. National Research Council: Precision Agriculture in the 21st Century. National Academy of Sciences: Washington D.C.

NUE. 2008. Facts and Figures Concerning Nitrogen Use Efficiency. Accessed 4/22/2008. Available at: http://nue.okstate.edu/NUE_Facts.htm

Rabalais, N.N., R.E. Turner, D. Justic, Q. Dortch, W.J. Wiseman Jr. and B.K. Sen Gupta. 1996. Nutrient changes in the Mississippi River and system responses on the adjacent continental shelf. Estuaries. 19:366–407.

Raun, W.R., J.B. Solie, G.V. Johnson, M.L. Stone, R.W. Whiney, H.L. Lees, H. Sembiring, and S.B. Phillips. 1998. Micro-variability in soil test, plant nutrient, and yield parameters in bermudagrass. Soil Science Society of America Journal. 62:683-690.

Raun, W.R. and G. V. Johnson. (1999). Improving nitrogen use efficiency for cereal production. Agronomy Journal 91:357–363.

Raun W.R., J.B. Solie, M.L. Stone, D.L. Zavodny, K.L. Martin, and K.W. Freeman. (2004). Automated calibration stamp technology for improved in-season nitrogen fertilization. Agronomy Journal. 97:338-342.

Raun W.R., J.B. Solie, M.L. Stone , K.L. Martin, K.W. Freeman, R. Mullen, H. Zhang, J.S. Schepers, and G.V. Johnson. 2005a. Optical sensor-based algorithm for crop nitrogen fertilization. Communications in Soil Science and Plant Analysis. 36:2759-2781.

Raun, W.R., J.B. Solie, K.W. Freeman, M.L. Stone, G.V. Johnson, and R.W. Mullen. 2005b.Growth stage, development, and spatial variability in corn evaluated using optical sensor readings. Journal of Plant Nutrition 28:173-182.

Russo, D. and W.A. Jury. 1987. A theoretical study of the estimation of the correlation scale in spatially variable fields. 1. Stationary fields. Water Resour. Res. 23, 1257–1268.

Sembiring, H., H.L. Lees, W.R. Raun, J.B. Solie, M.L. Stone, G.V. Johnson, E.V. Lukina, D.A. Cossey, J.M. LaRuffa, C.W. Woolfold, S.B. Phillips, and W.E. Thomason. 2000. Effect of growth stage and variety on spectral radiance in winter wheat. Journal of Plant Nutrition. 23:141-149.

Solie J.B., W.R. Raun, R.W. Whiney, S.L. Taylor, and J.D. Ringer. 1996. Optical sensor based filed element size and sensing strategy for nitrogen application. Transactions ASAE. 39. 6:1983-1992.

Solie J.B., W.R. Raun, and M.L. Stone. 1999. Submeter spatial variability of selected soil and plant variables. Soil Sci. Am. J. 63:1724-1733.

Solie J.B., M.L. Stone, W.R. Raun, G.V. Johnson, K. Freeman, R. Mullen, D.E. Needham, S. Reed, and C.N. Washmon. 2002. Real-time sensing and N fertilization with a field scale GreenSeeker[tm] applicator. Available at: http://nue.okstate.edu/Papers/Minnesota_2002_Solie.htm

Stone, M.L., J.B. Solie, W.R. Raun, R.W. Whiney, S.L. Taylor, and J.D. Ringer. 1996. Use of spectral radiance for correcting in-season fertilizer nitrogen deficiencies in winter wheat. Transactions ASAE, 39. 5:1623-1631.

Taylor, S.L., M.E. Payton, and W.R. Raun. 1999. Relationship between mean yield, coefficient of variation, mean square error and plot size in wheat field experiments. Communications in Soil Science and Plant Analysis. 30:1439-1447.

Teal, R.K., B. Tubana, K. Grima, K. Freeman, D. Arnall, O. Walsh, and W.R. Raun. 2006. In-Season prediction of corn grain yield potential using normalized difference vegetation index. Agronomy Journal. 98:1488-1496.

Turner, R.E. and N.N. Rabalais. 1994. Coastal eutrophication near the Mississippi river delta. Nature. 368:619–621.

Western, A.W., and G. Bloschl. 1999. On the spatial scaling of soil moisture. J. Hydrol. (Amsterdam) 217:203–224.

CHAPTER III

FORMULATION OF AN ANALYTICAL RELATIONSHIP BETWEEN NDVI, VARIANCE, AND FRACTIONAL VEGETATIVE COVER IN SUB-PLOT SAMPLING

Abstract

Accurate estimation of fractional vegetative cover (FVC) is difficult because of the coarse resolution of most imagery. Spectral mixture analysis (SMA) is a common method of describing FVC that assumes each pixel, or sensing frame, is a linear combination of characteristic spectral types (e.g. soil, water, plant, shadow, etc.) called endmembers. For SMA to accurately estimate FVC, it is essential that the endmembers be chosen correctly according to the depth and dimension of the imagery. This paper shows that endmember selection can be performed using the relationship of sub-plot mean and variation of normalized difference vegetative index (NDVI) imagery. This research found that a quadratic relationship (R^2 >0.56) exists between mean plot NDVI and plot variance. Since endmembers should have consistent homogeneity and low variance, the roots of the quadratic relationship provide endmember estimates of bare soil (N_s) and complete plant coverage (N_c). This research further demonstrates analytically and empirically that FVC = 50% occurs at the vertex (highest variance) of the sub-plot mean NDVI and variance relationship. This methodology demonstrates a simple and accurate in-field method of estimating FVC for sensors capable of sub-plot sampling.

Introduction

It has long been a goal of remote sensing to accurately estimate fractional vegetative cover (FVC) from spectral information. Complete vegetative cover is the part of vegetative canopy where no bare soil is detected (Carlson and Ripley 1997). Commonly, transformations of the normalized difference vegetative index (NDVI) are used to estimate FVC. However, the coarse nature of most imagery precludes accurate estimates of FVC (Xiao and Moody 2005). Commonly, spectral mixture analysis (SMA), a general linear additive model, is used to estimate FVC from multispectral imagery (Xiao and Moody 2005).

Spectral mixture analysis is based on the assumption that a single image pixel is a combination of various spectral types, such as vegetation, soil, shadow, water, etc. multiplied by its fractional cover. Pixel reflectance, under the SMA assumption, is a linear combination of specific spectral types within the pixel called endmembers (Palaniswami 2006). Tompkins et al. (1997) gives a general equation for SMA model assumptions. SMA is a linear combination of endmembers and fractions of coverage

$$R_b = \sum_{i=1}^{m} f_i r_{ib} + E_b \tag{3.1}$$

where R_b is the aggregate pixel reflectance for band *b* for *m* endmembers, f_i is the fractional abundance of endmember *i*, r_{ib} is pixel reflectance in band *b* of endmember *i*, and E_b is the error in band *b*. This model is constrained by:

$$\sum_{i=1}^{m} f_i = 1 \tag{3.2}$$

where the sum of fractional coverage must equal 1.

The number of endmembers for SMA is dictated by the dimensionality (bands) of the image (Theseira et al. 2002) and should be equal to the number of independent bands (Small 2001; Theseira et al. 2002). Dennison and Roberts (2003a) point out that it is critical for SMA's accuracy that endmembers be chosen carefully.

Under SMA, each pixel in an image is composed of a combination of endmembers. This requires endmembers be estimated from the image, measured in laboratory settings, or in field experiments (Dennison and Roberts 2003b, Gutman and Ignatov 1998; Qi et al. 2000). This implies that endmembers are derived from samples of homogeneous pixel groups (e.g. forests, beaches, etc.). Xiao and Moody (2005) offer a key to within-image endmember selection; endmembers should have negligible spectral variance.

Arnall et al. (2006), based on previous research, suggested that coefficient of variation (CV) in combination with NDVI can improve prediction of plant density. Lukina et al (2000) found that the average CV of NDVI tends to decrease as vegetative coverage increases across a farm field. Weisz et al. (2001) found that as plant stand increased, yield increased and field variation decreased. These findings demonstrate that plant density (2-dimensional) is inversely proportional to variance and that a complete coverage endmember can be estimated from NDVI measurements of dense plant stands with low variance. However, using variance to estimate endmembers necessitates the uncommon ability of the sensor to sample sub-pixel.

The GreenSeeker^{TM} optical sensor (Ntech Industries, Ukiah CA.) developed by Oklahoma State University senses a 0.6m x 1cm area and is capable of sensing more than 10 samples per 0.4m^2 at 10 mph (Raun et al. 2005). This sensor type is able to

compartmentalize individual sub-plot readings where mean and standard variance estimates are available for each plot. Under this methodology a sensing plot is analogous to an image pixel. This lends the ability to analyze spectral mixtures and estimate endmembers without relying on identifying contiguous pixel groups in multiple bands.

Carlson and Ripley (1997) offer a two-endmember model to predict FVC from the NDVI of bare soil and complete plant coverage:

$$FVC = \left[\frac{N - N_s}{N_c - N_s} \right]^2 \tag{3.3}$$

where N is variable NDVI, N_s is NDVI of bare soil, and N_c is NDVI of complete plant coverage. Gutman and Ignatov (1998), however, prove a simpler SMA model can be used to relate FVC and NDVI for non-dense vegetation (e.g. Kerr et al. 1992; Gillies and Carlson 1995; Wittich and Hansing 1995; Valor and Caselles 1996). The SMA relationship shows NDVI to be a linear combination of bare soil (N_s) and complete coverage (N_c) with NDVI weighted by the percentage of vegetative cover (FVC), such that:

$$NDVI = FVC(N_c) + (1 - FVC)N_s \tag{3.4}$$

This SMA model assumes a linear form and can be easily transformed to estimate FVC by:

$$FVC = \left[\frac{N - N_s}{N_c - N_s} \right] \tag{3.5}$$

Where N is variable NDVI, N_s is bare soil and N_c is complete plant coverage.
Both models assume that NDVI and FVC are related by two endmembers based on bands used to calculate NDVI (red and near infrared). This major simplification allows FVC to be estimated directly from NDVI without multiple bands. For additional simplification,

Gutman and Ignatov (1998) reflect numerous authors who have shown that a non-linear relationship was not detectable in varying plant densities. The authors argued that a purely linear relationship did not significantly change the estimation error.

Lukina et al. (1999), using red-green-blue (RGB) digital imagery, found that NDVI was significantly linearly correlated (R^2>0.80) with vegetative coverage, such that NDVI was linearly regressed on percent vegetative cover (VC%):

$$\text{NDVI} = \beta_0 + \beta_1(\text{VC\%}) \tag{3.6}$$

Similar work by Jones et al. (2007) in spinach, using a multispectral imagery, found that biomass is related exponentially to NDVI (R^2 = 0.94) and that vegetative coverage by percent (VC%) is logarithmically related to biomass (R^2 = 0.91):

$$\text{Biomass} = ae^{c\text{NDVI}} \tag{3.7}$$

$$\text{VC\%} = d\ln(\text{Biomass}) \tag{3.8}$$

where a, c, and d are constants of regression.

The objective of this research is to empirically validate the relationship between NDVI and FVC. A review of the literature shows an inverse relationship between variance and NDVI collected in experimental plant stands, such that variance decreases as plant material increases. Previous experimentation suggests a similar inverse relationship between percent soil coverage and NDVI, such that variance is low in complete bare soil and increases as plant material increases. Taken in concert, these relationships imply a peak function where NDVI at minimum variance can be used as endmembers and maximum variance can be estimated at the vertex between bare soil and complete plant coverage.

Current literature suggests that a linear relationship exists between NDVI and FVC. The model supported by Gutman and Ignatov (1998) describes a method of estimating FVC using endmember bare soil (N_s) and complete plant coverage (N_c) as values derivable from the dataset. Consequent to this model is the estimation of 50% vegetative coverage being midway between N_s and N_c.

Specifically, this paper will show a quadratic relationship exists between sample standard deviation (Stdev) and mean NDVI and that the roots of this relationship provide estimates for N_s and N_c in the SMA model, where

$$\text{Stdev(NDVI)} = a\text{NDVI}^2 + b\text{NDVI} + c \tag{3.9}$$

with endmembers at the upper and lower roots:

$$\text{NDVI} = \frac{-b - \sqrt{b^2 - 4ac}}{2a} = \hat{N}_c \tag{3.10}$$

$$\text{NDVI} = \frac{-b + \sqrt{b^2 - 4ac}}{2a} = \hat{N}_s \tag{3.11}$$

Using N_s and N_c as constants in Equation 3.5 the vertex of the mean/variance relationship will occur at 50% vegetative cover, such that:

$$\text{FVC}\left(-b/2a\right) = \frac{\left(-b/2a\right) - \frac{-b + \sqrt{b^2 - 4ac}}{2a}}{\frac{-b - \sqrt{b^2 - 4ac}}{2a} - \frac{-b + \sqrt{b^2 - 4ac}}{2a}} = 0.5 \tag{3.12}$$

Methods and Materials

Data compiled for this research consists of sensor-based calibration stamp samples, vegetative coverage samples, and camera based experimental spinach trials. The field dataset is used to validate the results of a simulated remote sensing experiment.

In this study, mean NDVI, standard deviation of the mean, and corresponding FVC serve as primary metrics. Previous research suggests the use of the coefficient of variation (CV) because samples were being taken from different fields. However, CV becomes insensitive for means approaching zero and should only be used on true ratio data (Zar 1984). It is debatable whether NDVI represents true ratio data. For this reason Taylor et al. (1999) argued for the use of the mean square error (MSE) in preference to CV for instances where common units of measure were used in different treatments. Additionally, MSE, unlike CV, has the property of being the square of the experimental units – where the root mean square error (RMSE) is in comparable units. It is unclear if MSE is preferable over customary variance estimates when no comparison of samples is being made (e.g. analysis of variance). Conceptually, a simpler, more common method to determine variance in experimental units is preferable; for this reason the standard deviation is used in this study.

Because samples in this experiment are from sensor and camera based experiments, it is essential that NDVI be demonstrably uniform across sensor type. Research in Jones et al. (2007) shows that NDVI derived from GreenSeeker^{TM} sensors are highly linearly correlated ($R^2 = 0.97$) with NDVI derived from the multispectral camera (DuncanTech MS3100) used in this experiment. The similarity between sensors allows field collected samples to be validated by multispectral images.

To understand the systematic relationship between variance and NDVI, a 10x10 (100 element) value matrix was constructed in Splus 2000 (Insightful®) to simulate a typical plot sensing experiment. In each simulation run, elements in the matrix were uniform randomly assigned either complete plant coverage or bare soil binomial

identification (0 or 1) in accordance with FVC levels (0% - 100%) from Equation 3.4. The elements allocated to complete plant coverage (N_c) were assigned a random normal NDVI value with $Mean_{NDVI} = 0.85$ and $StDev_{NDVI} = 0.01$ and bare soil (N_s) $Mean_{NDVI} = 0.16$ and $StDev_{NDVI} = 0.02$. Complete plant coverage and bare soil NDVI mean and standard deviation values were derived from a continuous native grass experimental plot in another part of this study. A simulation consisted of 1000 value matrices at each FVC ranging in whole values 0% - 100% producing 10 mean/standard deviation values for each FVC level, where each value matrix was averaged by element across each column, simulating a perpendicular single sensor scan and then by row to calculate plot mean NDVI and standard deviation.

To confirm the relationship between the mean and standard deviation of within sample NDVI, 16 multispectral images of spinach plots, described in Jones (et al. 2007), were analyzed. The capture area for each image was constructed of 1.27cm (3/4in.) PVC pipe enclosing a 0.76m x 0.91m area. Images were collected by a DuncanTech MS3100 multispectral camera (Auburn, Cal.), sensing green, red, and near-infrared bands at 550, 670, and 780nm ($\pm$ 10nm), respectively. The 3-band images were calibrated and converted to NDVI images with MatLab (MathWorks, Inc., Natick, Mass.) software, using the standard reflectance NDVI calculation. However, because NDVI is theoretically bound between [-1,1], subsequent NDVI images with negative values were not set to zero as normal practice usually dictates in order to emphasize the distinction between bare soil and dense vegetation. Further, images were resampled to lower resolution by averaging to aid computation and reduce background noise. A 20 pixel kernel was used to decrease resolution because variogram analysis of these data showed a

30 - 50 maximum range indicating a 15 – 25 pixel zone of influence; thus half the maximum range was selected to minimize variance aliasing across scales (Russo and Jury 1987; Western and Bloschl 1999). From this aggregated image, a mean and standard deviation image was created by a 3 pixel square search kernel.

To delineate the relationship between 50% FVC and variance, 30 plots were sensed with the hand-held GreenSeeker™ across five vegetative coverage levels in a 2m x 10m continuous native grass experimental plot. The plot received 45 kg ha^{-1} pelleted 10-20-10 commercial fertilizer previous to growing season and had consistent NDVI ($NDVI_{Plant} = 0.85 \pm 0.01$) at the time of sensing. A wooden frame 61cm x 61cm was constructed as a sensing boundary. An initial NDVI sensing represented 100% vegetative cover. Then reflective panels ($NDVI_{Panel} = 0.16 \pm 0.02$), representing soil from the experimental area ($NDVI_{soil} = 0.159 \pm 0.013$), were placed in the frame and sensed to achieve 75%, 50%, 25%, and 0% vegetative coverage. The mean and standard deviation of experimental sample were calculated.

Validation at the field level was achieved by analyzing five sites sampled under a calibration stamp design (Raun et al. 2004), which is a 3m x 3m matrix of 9 – $1m^2$ plots, consisting of four check plots and five treatment level plots in wheat and bermudagrass. Each calibration stamp was sensed at $1m^2$ resolution with the hand-held GreenSeeker™ optical sensor. The sensor detects and records individual NDVI values every 0.6m x 1cm across the plot producing mean NDVI and standard deviations.

Results

Figure 3.1 demonstrates the simulated relationship between NDVI and standard deviation of NDVI with varied FVC and endmembers $N_s = 0.16 \pm 0.02$ and $N_c = 0.86 \pm 0.01$.

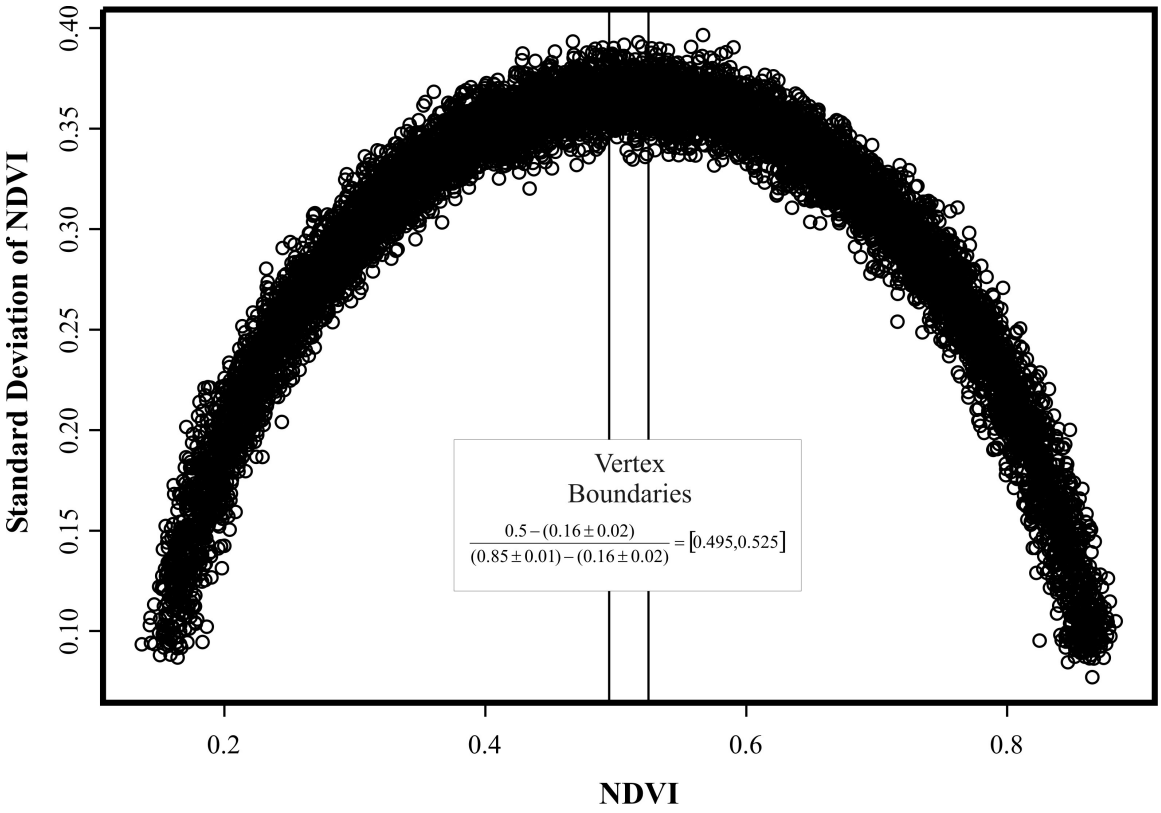

Figure 3.1: Simulated NDVI Versus Standard Deviation of NDVI (10,000 Simulation Runs) with Maximum Variance Estimation Bounds from Equation 3.5. NDVI = 0.86 and NDVI = 0.16 Used as Estimates of Complete Vegetative Coverage and Bare Soil, Respectively.

The relationship, Figure 3.1, shows the simulated standard deviation of NDVI is quadratically related to simulated mean NDVI and that minimum variance occurs at bare soil (≈ 0.16) and complete plant coverage (≈ 0.86) values. Conversely, maximum variance is centered between the endmembers and occurs within predicted bounds (0.495,0.525) from Equation 3.5.

Figure 3.2 shows the simulated relationship between varied levels (0%-100%) of FVC and standard deviation of NDVI.

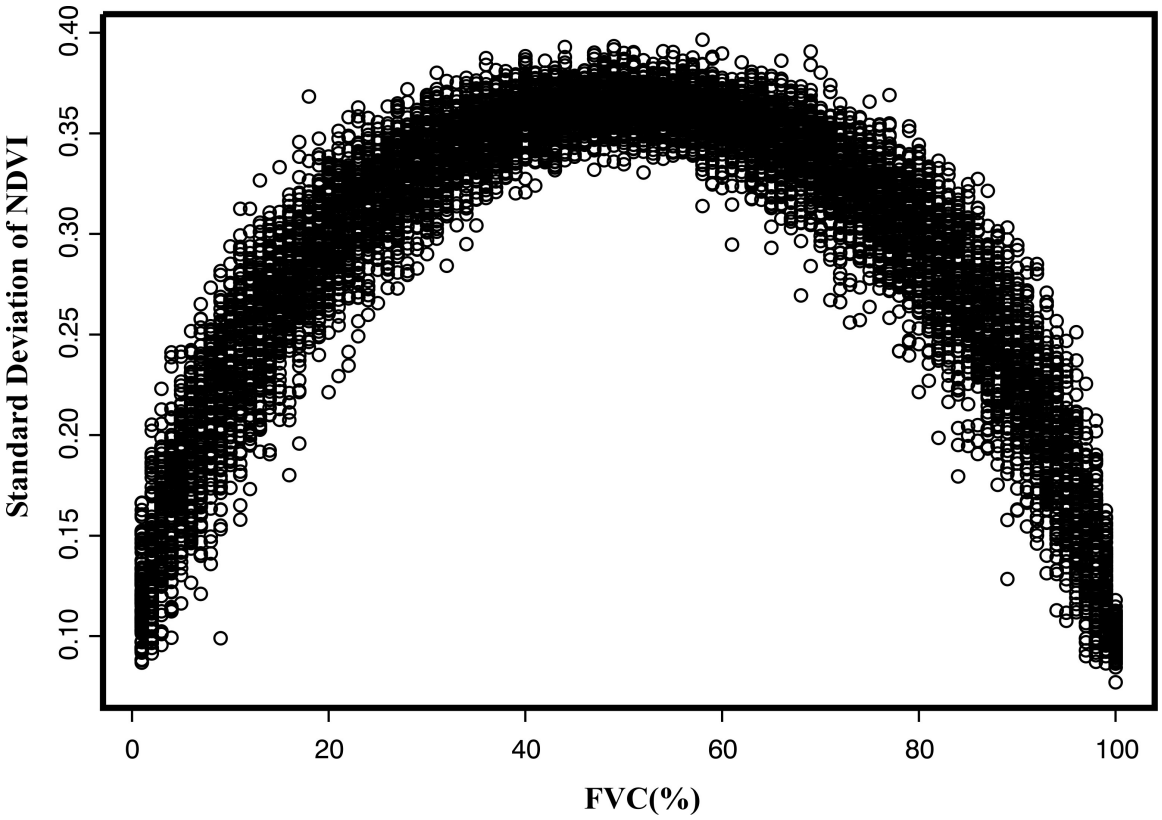

Figure 3.2: Simulated FVC(%) Versus Standard Deviation of NDVI (10,000 Simulation Runs) Where Maximum Variance Occurs at 50% FVC.

Figure 3.2 demonstrates that there is a predictable relationship between FVC and standard deviation. Variance is highest at 50% FVC and is minimized at 0% and 100% FVC. Attenuated data near minimum variance is due to the levels of FVC being chosen as discrete whole numbers and not continuous.

Figures 3.1 and 3.2 show that FVC and NDVI are quadratically related to the standard deviation of NDVI, such that $f(\text{FVC}) = \text{Stdev(NDVI)} = g(\text{NDVI})$ implying that the functions of FVC and NDVI are equal $f(\text{FVC}) = g(\text{NDVI})$. Therefore, using the

FVC transformation (Equation 3.5) and the roots of NDVI relationship (Equations 3.10 & 3.11) FVC and NDVI should have a linear relationship.

Figure 3.3 shows an example plot derived from the multispectral spinach imagery and is representative of the data distribution from this experiment.

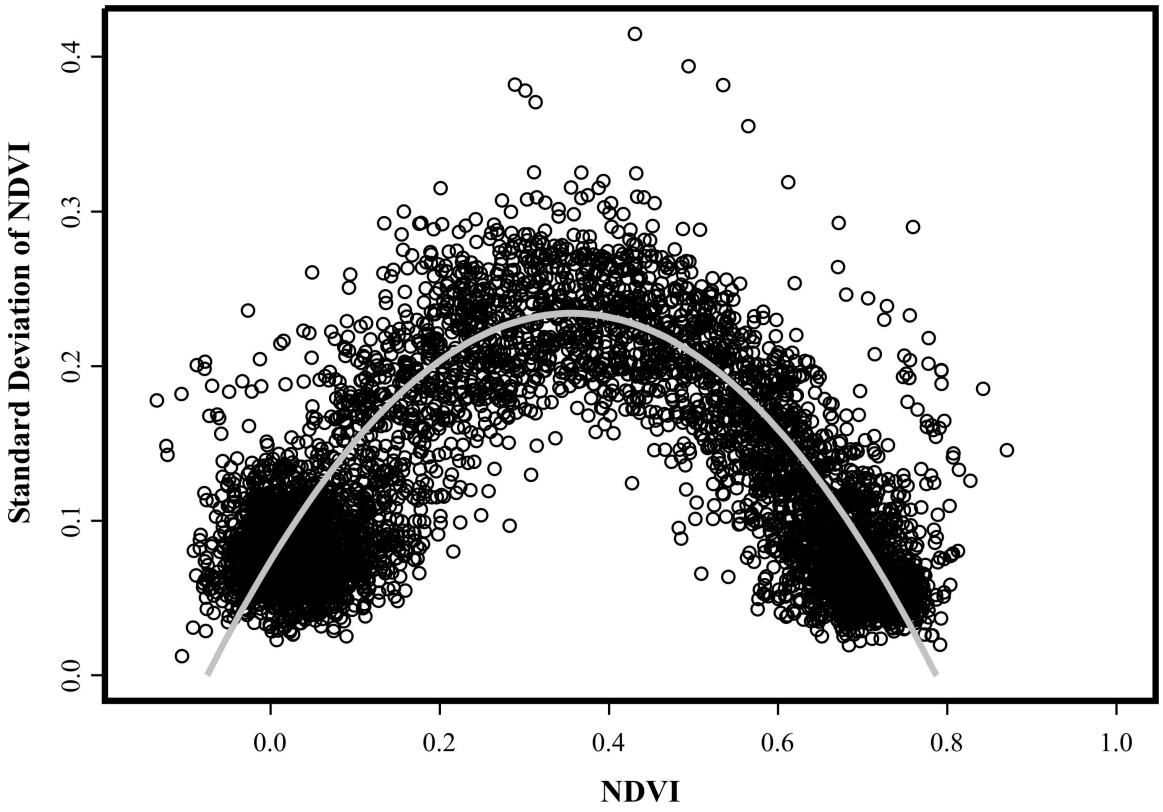

Figure 3.3: Spinach Imagery NDVI versus Standard Deviation of NDVI with Quadratic Regression Fit (Parameters Described in Table 3.11: Plot 1).

The relationship (Figure 3.3) demonstrates a quadratic response between mean NDVI and standard deviation confirming the initial assumptions made from simulation results.

Table 3.11 shows the parameters of a quadratic regression model used to estimate the relationship. The values are model coefficients (a, b, and c: Equation 3.9), coefficient of determination (R^2), coordinates of the maximum standard deviation (Xvert and Yvert), and the endmember estimates N_s (Lower Root) and N_c (Upper Root).

Table 3.1: Quadratic Regression Parameters for Spinach Dataset

Plot	a	b	c	R^2	Xvert	Yvert	Lower Root	Upper Root
Plot 1	-1.036	0.739	0.076	0.567	0.357	0.207	-0.091	0.804
Plot 2	-1.001	0.726	0.074	0.581	0.362	0.206	-0.091	0.815
Plot 3	-0.989	0.77	0.042	0.626	0.389	0.192	-0.052	0.829
Plot 4	-0.861	0.495	0.134	0.617	0.287	0.205	-0.201	0.775
Plot 5	-0.91	0.557	0.117	0.593	0.306	0.203	-0.166	0.777
Plot 6	-0.982	0.596	0.128	0.601	0.303	0.218	-0.168	0.775
Plot 7	-1.08	0.525	0.174	0.66	0.243	0.237	-0.226	0.712
Plot 8	-1.222	0.79	0.109	0.687	0.323	0.237	-0.117	0.763
Plot 9	-1.061	0.723	0.096	0.614	0.34	0.219	-0.114	0.795
Plot 10	-1.232	0.763	0.121	0.692	0.31	0.24	-0.131	0.75
Plot 11	-0.878	0.591	0.098	0.573	0.337	0.197	-0.137	0.81
Plot 12	-0.914	0.656	0.084	0.593	0.359	0.202	-0.111	0.829
Plot 13	-1.105	0.707	0.12	0.641	0.32	0.233	-0.139	0.779
Plot 14	-1.052	0.723	0.095	0.606	0.344	0.219	-0.113	0.8
Plot 15	-1.151	0.861	0.057	0.597	0.374	0.218	-0.061	0.81
Plot 16	-1.056	0.781	0.063	0.582	0.37	0.207	-0.073	0.813

Table 3.1: Model coefficients (a, b, and c: Stdev(NDVI) =aNDVI^2 +bNDVI +c), Coefficient of Determination (R^2), Coordinates of the Maximum Stdev(NDVI) (Xvert and Yvert), and Endmember Estimates N_s (Lower Root: Bare Soil) and N_c (Upper Root: Complete Vegetative Coverage).

Each regression demonstrated in Table 3.1 was significant ($P<0.01$) and returned reasonably high R^2 values (>0.56). Interestingly, predictions of N_s (Lower Root: Bare Soil) are consistently less than 0 for the imagery, demonstrating an instance where CV is not an appropriate measure of variance in this study. The extremely low bare soil NDVI values are likely due to a combination of extraneous factors such as soil texture, ambient moisture, and stark transition between plant material and bare soil.

Figure 3.4 shows the results of the native grass vegetative cover experiments. Here NDVI samples were taken across five levels of FVC (0%, 25%, 50%, 75%, and 100%).

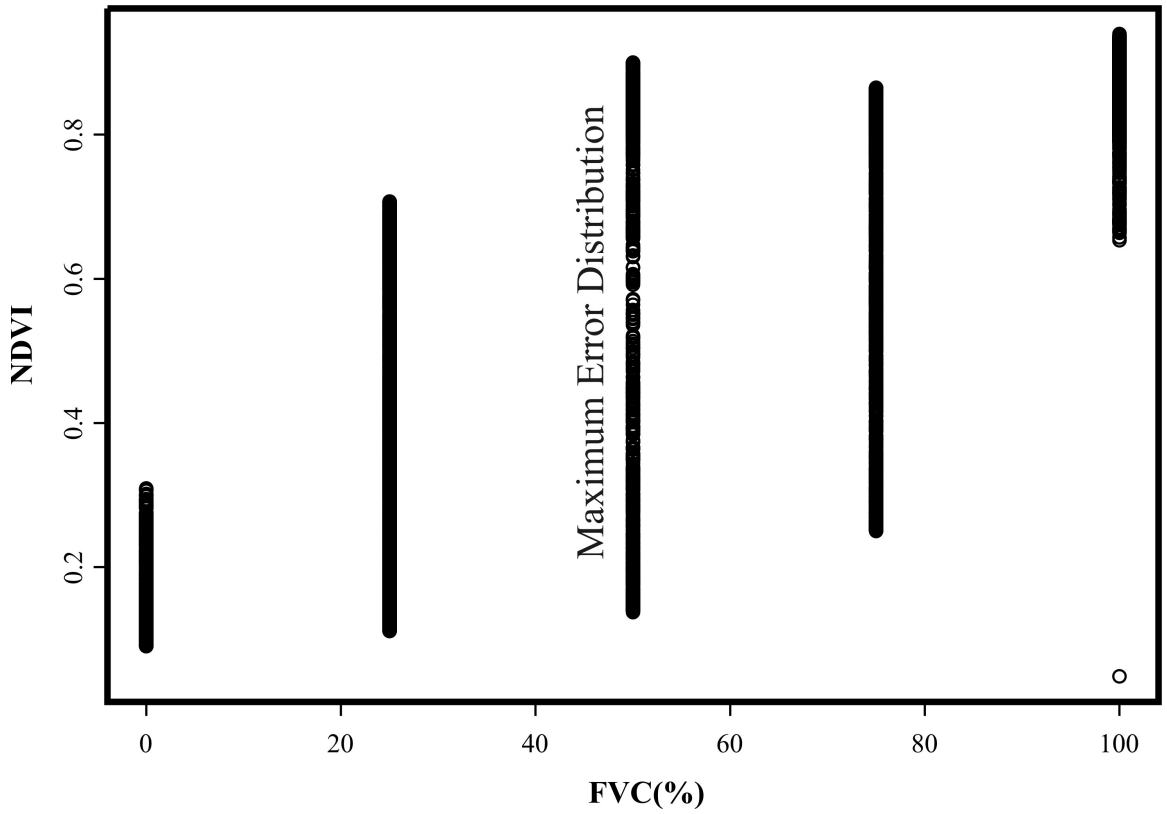

Figure 3.4: FVC (%) Versus NDVI from Native Grass Vegetative Coverage Experiment.

Figure 3.4 shows that NDVI is highly dispersed at FVC = 50% in comparison. In addition, variance is small at 0% and 100% FVC. Table 3.2 confirms that the standard deviation is highest at FVC= 50% and lowest at FVC = 0% & 100%.

Table 3.2: Standard Deviations for Levels of FVC (%)

FVC (%)	**0**	**25**	**50**	**75**	**100**
Standard Deviation	0.0442	0.1839	0.2662	0.1995	0.0565

This verifies complete bare soil and complete plant coverage should have fairly stable low variance (c.f. Xaio and Moody 2005) while equally mixed N_s and N_c should have maximum variance.

Figure 3.5 shows the results of field level research on calibration stamp plots, in wheat and bermudagrass where plot averaged NDVI is matched with corresponding variance.

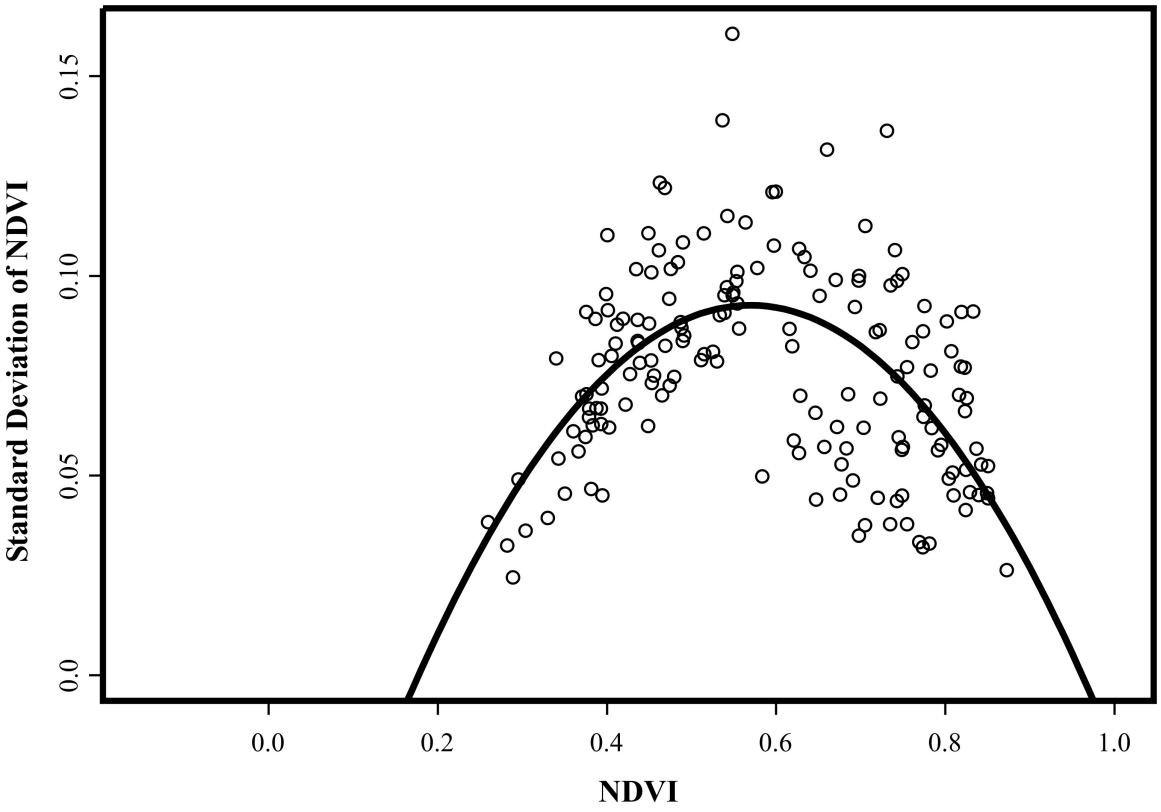

Figure 3.5: NDVI Versus Standard Deviation of NDVI for Calibration Stamp Design with Quadratic Regression Fit (see Table 3.3: Wheat and Bermudagrass "Combined").

Figure 3.5 shows a quadratic relationship between NDVI and standard deviation confirming previous findings. Specifically, this experiment demonstrates NDVI and variance are related even at increasingly larger measurement scales. Table 3.3 shows the regression parameters associated with this trial.

Table 3.3: Quadratic Regression Parameters for Calibration Stamp Dataset

Plot	a	b	c	R^2	Xvert	Yvert	Lower Root	Upper Root
Combined	-0.602	0.686	-0.103	0.316	0.569	0.093	0.177	0.962
Wheat	-0.729	0.868	-0.159	0.511	0.595	0.099	0.226	0.964
Bermuda	-0.836	0.837	-0.114	0.53	0.5	0.095	0.163	0.838

Table 3.3: Model coefficients (a, b, and c: Stdev(NDVI) =aNDVI^2 +bNDVI +c), Coefficient of Determination (R^2), Coordinates of the Maximum Stdev(NDVI) (Xvert and Yvert), and Endmember Estimates N_s (Lower Root: Bare Soil) and N_c (Upper Root: Complete Vegetative Coverage).

Regressions displayed in Table 3.3 were significant ($P<0.01$), but showed weak R^2 when species were combined although R^2 was improved when species were individually modeled. This is an intuitive finding because wheat and bermudagrass have significantly different canopy patterns and will consequently exhibit different variances. Dennison and Roberts (2003b) found that plant phenology contributed significant confusion in change detection using multiple endmember spectral mixture analysis (MESMA).

Figure 3.6 shows the simulated relationship between NDVI and FVC for estimated endmembers ($N_s = 0.16 \pm 0.02$ and $N_c = 0.86 \pm 0.01$).

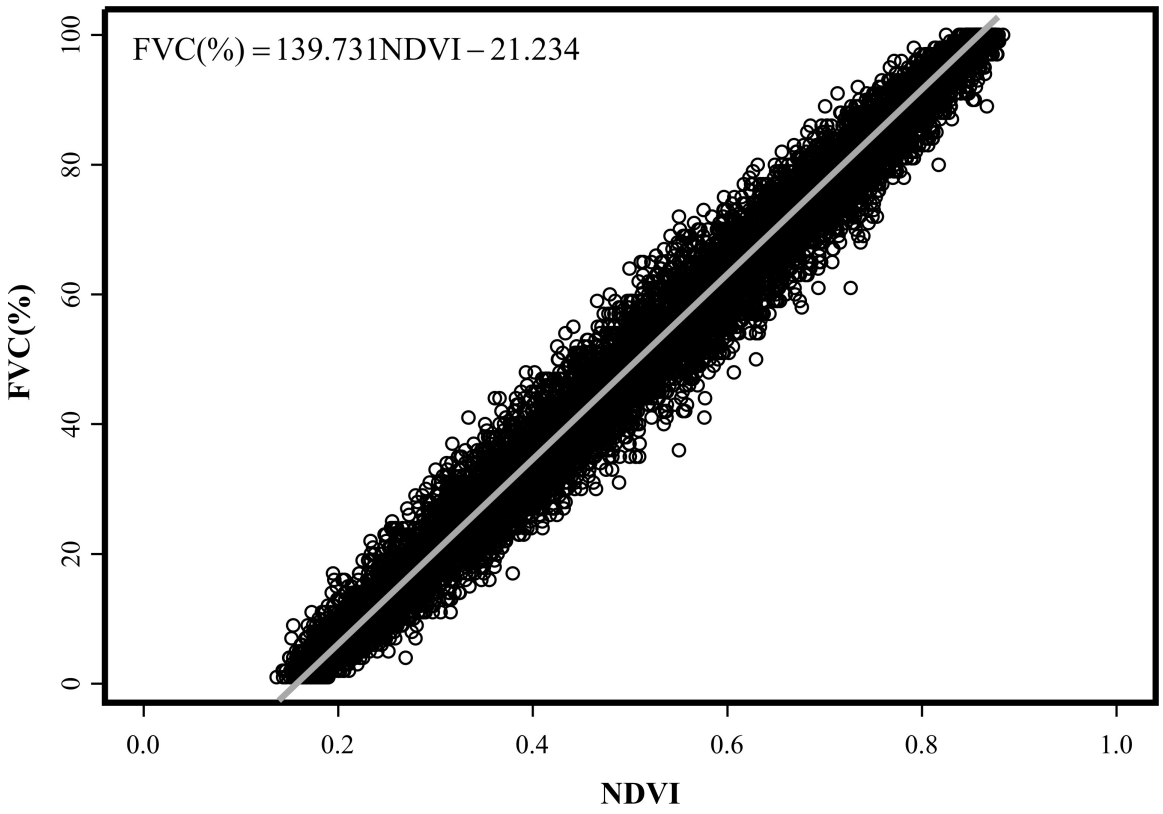

Figure 3.6: Simulated NDVI Versus FVC(%) (10,000 Simulation Runs) with Linear Regression Fit (Parameters in Table 3.4: "Simulation").

The simulation (Figure 3.6) exhibits a linear relationship between NDVI and FVC. Similarly, (Figure 3.7) shows the relationship between NDVI and FVC from the vegetative cover experiments in native grass stands.

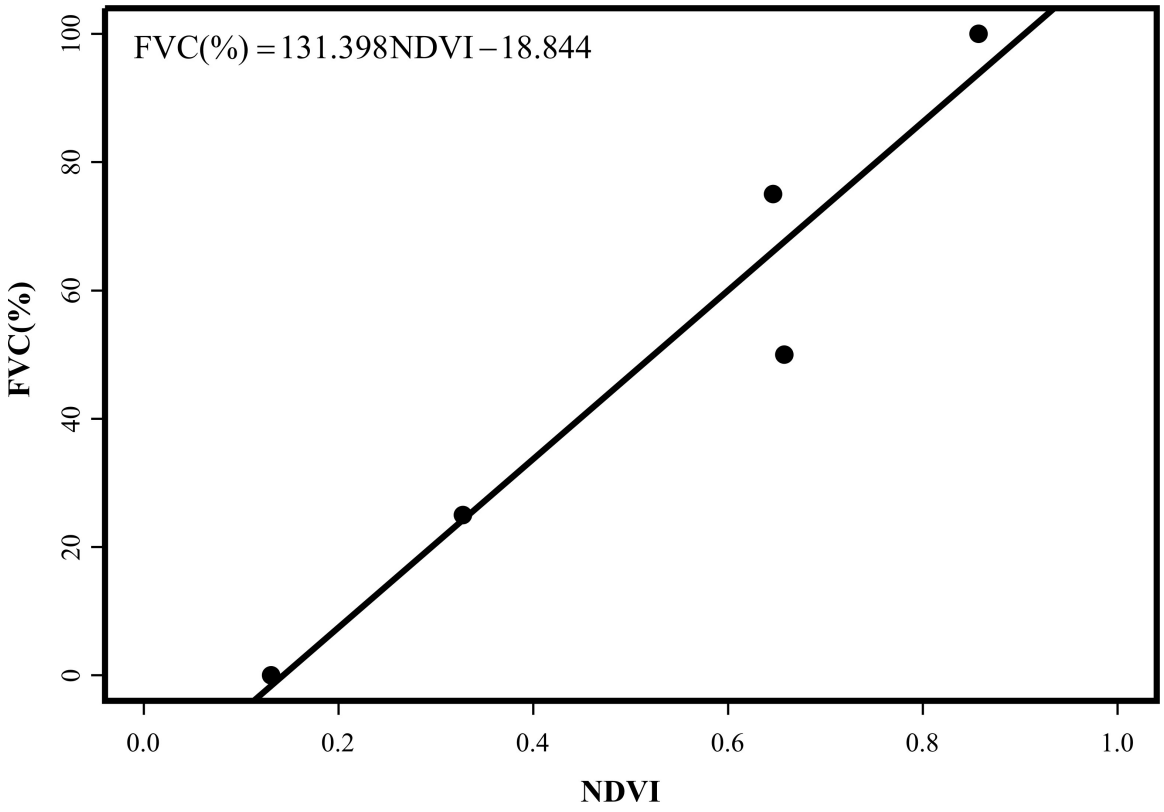

Figure 3.7: NDVI Versus FVC(%) from Native Grass Vegetative Cover Experiment with Linear Regression Fit (see Table4: "Field").

The linear nature of Figure 3.7 serves to validate the assumption of a linear relationship between NDVI and FVC. Table 3.4 shows the parameters and R^2 for the linear relationship between NDVI and FVC.

Table 3.4: Linear Regression Parameters for Simulated NDVI and Vegetative Cover Experiments.

Model	Intercept	Slope	R^2
Simulation	-21.234	139.731	0.978
Field	-18.844	131.398	0.931

Slope prediction was extended to experiments where FVC was not collected as a variable calculated by

$$\text{slope}_{FVC} = \frac{100}{N_c - N_s} \tag{3.13}$$

The spinach imagery has an average slope (109.483) and the calibration stamp experiments have an average slope (137.001). Earlier work by Lukina et al. (1999) showed commensurate average slopes at (158.019).

Discussion

Results from the simulation indicate a quadratic relationship between NDVI and plot variability. This relationship appears to be a product of the FVC within the plot area. Given the nature of this relationship, NDVI of bare soil (N_s) and complete vegetative cover (N_c) will have low variation since these areas are uniform. As uniformity decreases variance increases until a maximum is reached at a predicted equal mixture of N_s and N_c.

Multispectral imagery confirms a quadratic relationship for extremely fine resolution with relatively good correlation ($R^2 > 0.57$). Given this relationship, it is reasonable that N_s and N_c can be estimated by the roots (zeros) of the quadratic regression equation, albeit the bare soil estimates tended to be extremely low.

Selective vegetative cover experimentation in continuous native grass stands shows that variation of NDVI is highest at 50% FVC. This experiment serves to confirm that maximum variance occurs at the vertex of the NDVI-variance relationship and validates the derivation of Equation 3.12 showing that FVC = 50% occurs at the vertex.

Results from the calibration stamp design show the characteristic quadratic relationship between NDVI and variance. This finding suggests that the same overall relationship may exist at a field-level scales. Further, this experimentation hints that species, by virtue of canopy structure, affect variance and ultimately estimates of bare soil and complete coverage. This is confirmed with the spinach imagery where stark differences between soil and plant material resulted in negative NDVI estimates for bare

soil. Additionally, the comparison of wheat and bermudagrass showed that canopy structure affects the variability. Further research should be conducted to determine if the definitions of bare soil and complete vegetative coverage NDVI are site specific.

Lastly, both simulation and field research confirm the linear relation of NDVI to FVC found in the literature. Subsequent application of this finding to experiments that did not capture FVC necessitated a slope function (Equation 3.13) and showed commensurate slopes across all data sets. This result confirms the linear relationship between NDVI and FVC suggested in Gutman and Ignatov (1998: Equation 3.5) and Lukina et al. (1999: Equation 3.6). Additionally, Jones et al. (2007) showed that biomass is exponentially related to NDVI (Equation 3.7) and that vegetative coverage is logarithmically related to biomass (Equation 3.8). By combining these equations and solving for vegetative cover (VC%) in terms of NDVI an extrapolation of Jones et al. (2007) shows a linear relationship between VC% (FVC) and NDVI

$$VC\% = cdNDVI + d\ln(a) \tag{3.14}$$

where a, c, and d are constants from regression (Equations 3.7 and 3.8). In each of these cases the FVC line segment requires boundary values at FVC = 0 and FVC = 100, which can be derived from the roots of the standard deviation – NDVI relationship.

Conclusion

Findings from this study show that mean NDVI and variation in NDVI are related by a quadratic relationship. Further, this relationship can be used as a method of estimating NDVI of bare soil and complete vegetative cover endmembers (N_s and N_c) as the roots of the quadratic standard deviation-NDVI relationship. This mathematical relationship allows quantification of FVC at various levels of NDVI provided the

variance of NDVI is known. These findings, in concert with the spectral mixture analysis (SMA) model, show that FVC can be estimated in field by sub-sampling NDVI and calculating variance within plots.

References

Arnall, D.B., W.R. Raun, J.B. Solie, M.L. Stone, G.V. Johnson, K.Girma, K.W. Freeman, R.K. Teal, and K.L. Martin. 2006. Relationship between coefficient of variation measured by spectral reflectance and plant density at early growth stages in winter wheat. Journal of Plant Nutrition. 29:1983-1997.

Carlson, T.N. and D.A. Ripley. 1997. On the relation between NDVI, fractional vegetation cover, and leaf area index. Remote Sensing of Environment. 62:241-252.

Dennison, P.E. and D.A. Roberts. 2003a. Endmember selection for multiple endmember spectral mixture analysis using endmemeber average RMSE. Remote Sensing of Environment. 87:123-135.

Dennison, P.E. and D.A. Roberts. 2003b. The effects of vegetation phenology on endmember selection and species mapping in southern California chaparral. Remote Sensing of Environment. 87:295-309.

Gillies, R.R. and T.N. Carlson. 1995. Global data on land surface parameters for NOAA AVHRR for use in numerical climate models. Journal of Climate. 7:669-680.

Gutman, G. and A. Ignatov. 1998. The derivation of the green vegetation fraction from NOAA/AVHRR data for use in numerical weather prediction models. International Journal of Remote Sensing. V19. 8:1533-1543.

Jones, C.L., P.R. Weckler, N.O. Maness, R. Jayasekara, M.L. Stone, and D. Chrz. 2007. Remote sensing to estimate chlorophyll concentration in spinach using multispectral plant reflectance. Transactions of the ASABE. 50(6):2267-2273.

Kerr, Y.H., J.P. Lagouarde, and J. Imbernon. 1992. Accurate land surface temperature retrieval from AVHRR data with use of an improved split-window algorithm. Remote Sensing of Environment. 41:197-209.

Lukina, E.V., M.L. Stone, and W.R. Raun. 1999. Estimating vegetation coverage in wheat using digital images. Journal of Plant Nutrition. 22(2):341-350.

Lukina, E.V., W.R. Raun, M.L. Stone, J.B. Solie, G.B. Johnson, H.L. Lees, J.M. LaRuffa, and S.B. Phillips. 2000. Effect of row spacing, growth stage, and nitrogen rate on spectral irradiance in winter wheat. Journal of Plant Nutrition. 23(1):103-122.

Palaniswanmi, C., A.K. Upadhay, and H.P. Maheswarappa. 2006. Spectral mixture analysis for subpixel classification of coconut. Current Science. 91(12):1706-1711.

Qi, J.,Marsett, R.C., Moran, M.S., Goodrich, D.C., Heilman, P., Kerr, Y.H., Dedieu, G., Chehbouni, A., and X.X. Zhang. 2000. Spatial and temporal dynamics of vegetation in the San Pedro River basin area. Agricultural and Forest Meteorology. 105:55-68.

Raun W.R., J.B. Solie, M.L. Stone, D.L. Zavodny, K.L. Martin, and K.W. Freeman. 2004. Automated Calibration Stamp Technology for Improved In-Season Nitrogen Fertilization. Agronomy Journal. 97:338-342.

Raun W.R., J.B. Solie, M.L. Stone , K.L. Martin, K.W. Freeman, R. Mullen, H. Zhang, J.S. Schepers, and G.V. Johnson. 2005. Optical sensor-based algorithm for crop nitrogen fertilization. Communications in Soil Science and Plant Analysis. 36:2759-2781.

Russo, D. and W.A. Jury 1987. A theoretical study of the estimation of the correlation scale in spatially variable fields. 1. Stationary fields. Water Resour. Res. 23, 1257–1268.

Small, C. 2001. Estimation of urban vegetation abundance by spectral mixture analysis. International Journal of Remote Sensing. 22:1305-1334.

Taylor, S.L., M.E. Payton, and W.R. Raun. 1999. Relationship between mean yield, coefficient of variation, mean square error and plot size in wheat field experiments. Communications in Soil Science and Plant Analysis. 30:1439-1447.

Theseira, M.A., G. Thomas, and C.A.D. Sannier. 2002. An evaluation of spectral mixture modeling applied to a semi-arid environment. International Journal of Remote Sensing. 23:687-700.

Tompkins, S., J.F. Mustard, C.M. Pieters, and D.W. Forsyth. 1997. Optimization of endmembers for spectral mixture analysis. Remote Sensing of Environment. 59:472-489.

Valor, E. and V. Caselles. 1996. Mapping land surface emissivity from NDVI: Application to European, African, and South American areas. Remote Sensing of Environment. 57:167-184.

Weisz, R., C.R. Crozier, and R.W. Heiniger. 2001. Optimizing nitrogen application timing in no-till soft red winter wheat. Agronomy Journal. 93:435-442.

Western, A.W., and G. Bloschl. 1999. On the spatial scaling of soil moisture. J. Hydrol. (Amsterdam) 217:203–224.

Wittich, K. and O. Hansing. 1995. Area-averaged vegetative cover fraction estimated from satellite data. International Journal of Biometeorology. 38:209-215.

Xiao, J. and A. Moody. 2005. A comparison of methods for estimating fractional green vegetation cover within a desert-to-upland transition zone in central New Mexico, USA. Remote Sensing of Environment. 98:237-250.

Zar, J.H. 1984. Biostatistical Analysis. 2nd ed. PrenticeHall, Inc. Englewood Cliffs, N.J.

CHAPTER IV

A SIGMOIDAL MODEL TO PREDICT YIELD POTENTIAL INCORPORATING CROP RESPONSE TO SUPPLEMENTAL NITROGEN

Abstract

Prediction of yield potential is central to Nitrogen (N) conservation efforts. Supplemental N applied in uniform blanket application neglects natural field variability demonstrated by varying plant response to supplemental N and idealistic yield goals assuming uniformity of return. Continual over application compounds environmental degradation and, as N fertilizer price increases, contributes to decline in agricultural profitability. However, recent advances in yield potential prediction and detection of plant N sensitivity offer improved management strategies. This research proposes a sigmoidal approach to accepted exponential yield potential models by incorporating a continuous plant response parameter. The sigmoid model, built from assumptions in current literature, is within 6% (for large samples) equitability with the current exponential model in reducing residual sum of squares. However, the sigmoidal approach ensures agronomic assumptions are maintained without a piece-wise defined model. This methodology translates supplemental N sensitivity to differential yield potential, especially for varied physical/chemical conditions and N application rate differences. This methodology also opens the way for economic analysis of yield potential gain for a cost reduction based approach to variable rate application.

Introduction

For many years Nitrogen (N) has been applied in farm fields as a low cost, easy-to-implement method to maximize yield. Blanket application of uniform, usually high rate, N disregards field variability, over-treats areas at N sufficiency, and subsequently results in excess N entering the environment. Agricultural pollution, especially lost N, besides being an aqueous pollutant, is borne by the farmer as a loss in productivity, and in concert with recent fertilizer price increases, 130% between 2000 and 2006 (Huang, 2007), is exacerbating the cost of N loss and leading to an intractable future for cropping systems. However, recent developments in variable rate theory and technology may stem future issues by matching application to in-field need.

Nitrogen use efficiency (NUE) provides an estimate of field N requirement by demonstrating the proportion of N returned in harvested product to N application. Therefore, the primary issue in increasing NUE centers on the effectiveness of supplemental N, since N contained in the harvest product is generally constant. Excessive N application, well above sufficiency, artificially lowers NUE. NUE is, therefore, predicated on a combination of residual N in the plant/soil matrix and applied N. To assess the effectiveness of N supplementation, given residual N concentrations, Johnson (2000) proposed the use of $RI_{Harvest}$. This index is the ratio of yield from N treated plots and untreated plots. Later Mullen et al. (2003) proposed a ratio of normalized difference vegetative index (NDVI) values from N treated and untreated plots as a mid-season estimate of $RI_{Harvest}$. Raun et al. (2005) developed a method to calculate N application rates from NDVI based on yield potential using RI_{NDVI} as a constant multiplier to augment the relationship for N treated plots, which meant RI_{NDVI} could be

calculated from the ratio of N treated and non-treated potential yields. Raun et al. (2005) further show that NDVI is exponentially related to yield potential within a specified interval of NDVI and increases with increasing NDVI until constrained under a maximum environmental cap (YP_{Max}). In this way, YP_{Max} represents maximum yield obtainable given ambient physical and chemical field conditions. Plant response to supplemental N (RI_{NDVI}) is, therefore, used as a constant multiplier to drive the Yield-NDVI curve to YP_{Max} quicker for low NDVI when plants show significant response (RI>1). Under this methodology yield potential is exponentially related to field rate NDVI given by:

$$YP_N = a(RI_{NDVI})e^{b(NDVI)} \text{ for : } YP_N < YP_{Max}; RI_{NDVI} = 1 \text{ for } N = 0 \qquad (4.1)$$

where yield potential (YP_N) is a function of field rate NDVI and plant response due to N application rate (RI) ranging between 0 kg N $ha^{-1}$and sufficient concentrations. Obviously, 0-N application results in no complementary plant response (RI=1), however RI is allowed to increase proportionately to increases in N application rate, which increases the overall function. Additionally, this function based methodology estimates YP_{Max} as the maximum yield obtainable with N sufficiency and is not defined for values less than NDVI = 0.25, which Raun et al. (2005) describes as the soil/crop divide. Plant response to supplemental N (RI_{NDVI}) can be found from the yield potential, where RI_{NDVI} is constant until YP_{Max}, inverse exponential until NDVI = 0.73, and asymptotically to $RI_{NDVI} \rightarrow 1$ after NDVI = 0.73.

However, evaluating RI at smaller than average (1m) measurement scale, referred to as fundamental field element scale (Solie et al. 1996; Raun et al. 1998; Solie et al.1999), Monroe et al. (2008) found that RI_{NDVI} is a continuous function inversely

proportional to residual N, such that as residual N increases to sufficiency, evidenced by increasing NDVI, subsequent plant response (RI_{NDVI}) decreases. They further found, by specifying asymptotic boundary conditions, that this process can be estimated as a two parameter inverse hyperbolic cosine model:

$$RI_{NDVI} = \frac{A_0(FpNDVI)}{\cosh(A_1 FpNDVI)} + 1 \quad (4.2)$$

where A_0 determines maximum RI_{NDVI} and A_1 is the rate at which plant sensitivity to N supplementation decreases as farmer practice NDVI (FpNDVI) increases. Maximum response is achieved at low NDVI because N is the primary limiting nutrient; however, as NDVI increases (healthier plant stands) response to supplemental N decreases. The rate of decreasing response, between maximum response and complete N sufficiency, determines the intensity of N limitation. In context of the model, lower parameter values indicate plots where N is constantly a primary limiting factor, whereas higher parameter values indicate plots where N is a primary factor for extremely low NDVI but is subordinated quickly as NDVI increases.

Raun et al. (2005) laid the groundwork by devising a yield potential (YP_0) model to predict yield using NDVI readings and noted several axiomatic constraints, such as plant sensitivity to supplemental N, exponential increase, and asymptotic extremes. Furthermore, their work advocates a maximum yield boundary (YP_{Max}), which has not been adopted in the YP_0 model as a parameter. Additionally, recent research suggests that RI_{NDVI} is a predicable continuous function as opposed to a piece-wise defined model.

The objective of this study is to construct a continuous yield potential (YP) model subject to constraints from recent findings and compliant with necessary boundary conditions to compare with field-collected data. This work contends a sigmoidal model

approach can incorporate axioms from Raun et al. (2005) and continuous plant response to N (Monroe et al. 2008) into a single coherent model able to predict yield potential from mid-season measurements. Benefits of such a model include economic decision making in treating with variable N application and marginal net benefits from treating intervals of NDVI.

Methods and Materials

Raun et al. (2005) show that yield potential is asymptotic for upper and lower NDVI values, specifically for NDVI $\rightarrow$NDVI at YP_{Max} and NDVI < 0.25. Additionally, they show field sampled NDVI is exponentially related to yield from those samples. Taken in concert, these findings imply a sigmoidal transition of asymptotically low yield for low NDVI, increasing exponentially through mid-range NDVI, and asymptotic yield at YP_{Max} for NDVI $\rightarrow$ 1.

Sigmoidal models are prevalent in biological fields as models of constrained growth and decay. Tsoularis and Wallace (2002) demonstrate that most sigmoidal models in use today are versions of the earlier Verhulst (1838) logistic model used to predict Malthusian growth. Logistic models are characterized by an initial population (initial asymptotic value), transition zone, and a "saturation level" population (carrying capacity) (Tsoularis and Wallice 2002; pg. 22) such that:

$$y = \frac{c}{1 + e^{-k(x-inf)}} \tag{4.3}$$

where *c* is the carrying capacity, *k* is a parameter of curvature, and *inf* is the point of inflection (center of transition).

In the case of yield represented in the NDVI domain, NDVI = 0 should result in YP = 0 as an initial condition and NDVI = 1 should result in YP = YP_{Max} at carrying

capacity. Of the models present in the literature, a logistic appears to be the best for this application, because the numerator contains a carrying capacity parameter, the model can have a zero lower asymptote, and the inflection point (*inf*) can be directly estimated.

For the model to represent field conditions it must be sensitive to plant response to supplemental N. Raun et al. (2005) verified that the model must transition to YP_{Max} quicker under N supplementation. Therefore, the exponent should comprise a measure of plant response (RI) to N supplementation for yield potential (YP_N), such that: $-k(NDVI*RI-Inf)$ where *k* is a regression estimated parameter of curvature, NDVI is the domain, RI is the variable measuring plant response to supplemental N, and *Inf* is the non-linear regression estimated inflection point. If the plant stand is not N treated (YP_0) then RI = 1 and the exponent reduces to $-k(NDVI-Inf)$. Thus yield potential is changed by N supplementation where N treated yield potential

$$YP_N = \frac{YP_{Max}}{1+e^{-k(NDVI*RI-inf)}} \quad (4.4)$$

is augmented by RI_{NDVI} and untreated stands are static at RI_{NDVI} =1

$$YP_0 = \frac{YP_{Max}}{1+e^{-k(NDVI-inf)}} \quad (4.5)$$

Data for this study came from six years (1998 – 2003) of yield monitoring in Hard Red Winter Wheat. This dataset included 700 yield (Mg ha^{-1}), pre-plant N rate (kg N ha^{-1}), and NDVI combinations across six years sensed at Feekes stage 4 – 6. Only 0 kg N ha^{-1} pre-plant rates were included in this study to observe base level YP_0 and to fit with parameters in the continuous RI_{NDVI} model (Monroe et al. 2008). As pre-plant N rate increases, residual N in the plant-soil matrix at also increases; therefore response to further supplemental top-dress N decreases. These data were evaluated separately by

year because RI is variable year to year (Raun et al. 2005) and yield is independent of previous years (Johnson and Raun 2003).

Response index (RI_{NDVI}) parameter values were taken from Monroe et al. (2008) and used to adjust the baseline yield curve. Parameters from this source were a composite of several experimental areas and designs at various growth stages. However, varied N rate application experiments in a calibration stamp design were specifically separated and analyzed for this study to show yield model adjustment for different N application rates. The calibration stamp design (Raun et al. 2004) is a 3m x 3m matrix of 9 – $1m^2$ plots, consisting of four check plots and five treatment level plots. Application rates were 22, 45, 67, 90, and 112 kg N ha^{-1} (20, 40, 60, 80, and 100 lbs N $acre^{-1}$) in wheat and bermudagrass. These experiments were conducted in 2004. Each calibration stamp was sensed at $1m^2$ resolution with the hand-held Greenseeker™ optical sensor (Ntech Industries, Ukiah CA.) The plots were sampled four times at intervals of two weeks after N application and averaged together.

Results and Discussion

To assess fit the proposed sigmoidal model is compared against the exponential model used in Raun et al. (2005) and compared by reduction of residual sum of squares (RSS). Figure 4.1 shows the comparison in model for 1998 yield values restricted to 0-N pre-plant application. Since YP_{Max} is an unknown saturation value describing the capacity of yield; it was first estimated as one standard deviation of yield plus maximum yield from the dataset. After the sigmoidal model was regressed, YP_{Max} was adjusted and the sigmoidal model was reparameterized iteratively until a minimum RSS was attained.

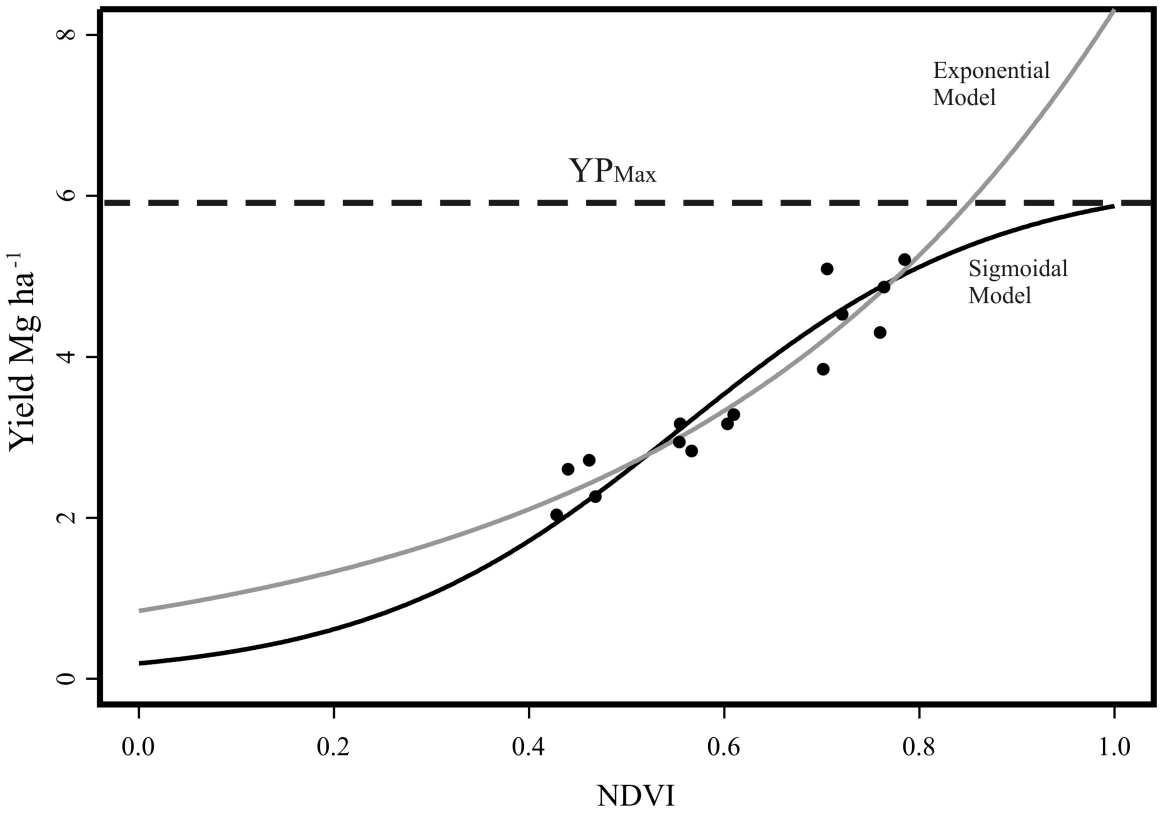

Figure 4.1: Regression Fit for1998 NDVI Verses Yield (Mg ha^{-1}) at 0 N Pre-Plant.

Figure 4.1 demonstrates that both models equitably pass through the main distribution of data. However, the exponential model continues unbounded after YP_{Max} is reached. The sigmoidal model maintains the exponential nature of these data and offers asymptotic boundary conditions such that YP_0 is obtained at NDVI = 0 and YP_{Max} is obtained at NDVI = 1. The sigmoidal model, a symmetric logistic, should reach the maximum value (YP_{Max}) at NDVI = 1 unless constricted by fitted parameters from the dataset. In this case, several trials show the sigmoidal model is overparameterized if YP_{Max} is estimated in the model. Therefore, YP_{Max} was adjusted outside the regression fit to ensure the sigmoidal model reached YP_{Max} at NDVI = 1.

Table 4.1 shows the parameter estimates and residual sum of squares (RSS) for the sigmoid and exponential models by year derived through non-linear least squares regression (Gauss – Newton method).

Table 4.1: Parameter and Fit (RSS) Comparison Between Sigmoidal and Exponential Model by Year.

	Sigmoid (Equation 6)			Exponential (Equation 1)			
Year	**k**	**inf**	**RSS**	**a**	**b**	**RSS**	**N samples**
1998	7.3141	0.5218	7.3734	0.3833	2.8063	7.8204	131
1999	3.9520	0.6253	9.5752	0.4380	2.0269	9.6883	125
2000	3.5853	0.5467	9.367	0.7409	1.6940	9.0453	128
2001	3.8885	0.5118	11.3792	0.7528	2.0350	10.7915	145
2002	1.8126	0.4744	49.2231	1.5349	0.9255	49.2367	144
2003	7.0764	0.4909	1.8335	0.8440	2.2881	1.5348	27

Table 4.1: Comparison of Model Parameters Between Sigmoidal and Exponential Non-Linear Regression Fitting by Year: k=Parameter of Curvature (Equation 6), inf = Inflection Point (Equation 6), a = Exponential Parameter (Equation 1), b = Exponential Parameter (Equation 1), RSS = Residual Sum of Squares.

Table 4.1 shows that there are consistently minor differences in RSS between models confirming fit equitability. For 1998, 1999, and 2002 the sigmoidal model reduced the RSS, while 2000, 2001, and 2003 it increased RSS. With the extremely small difference in RSS values (<6% for 1998 – 2002) it appears the sigmoidal model is reasonably well-suited to fit the data distribution as the established exponential model. The higher percent difference in RSS for the sigmoidal model in 2003 (20%) is likely due to the sample size (27).

Raun et al. (2005) describes and validates the process by which the yield potential curve is left shifted by implementation of constant response index (RI_{NDVI}). In summary, yield potential is shifted to YP_{Max} at lower NDVI by N supplementation. Figure 4.2 shows the inclusion of continuous RI_{NDVI} (c.f. Monroe et al. 2008) applied to the sigmoidal model.

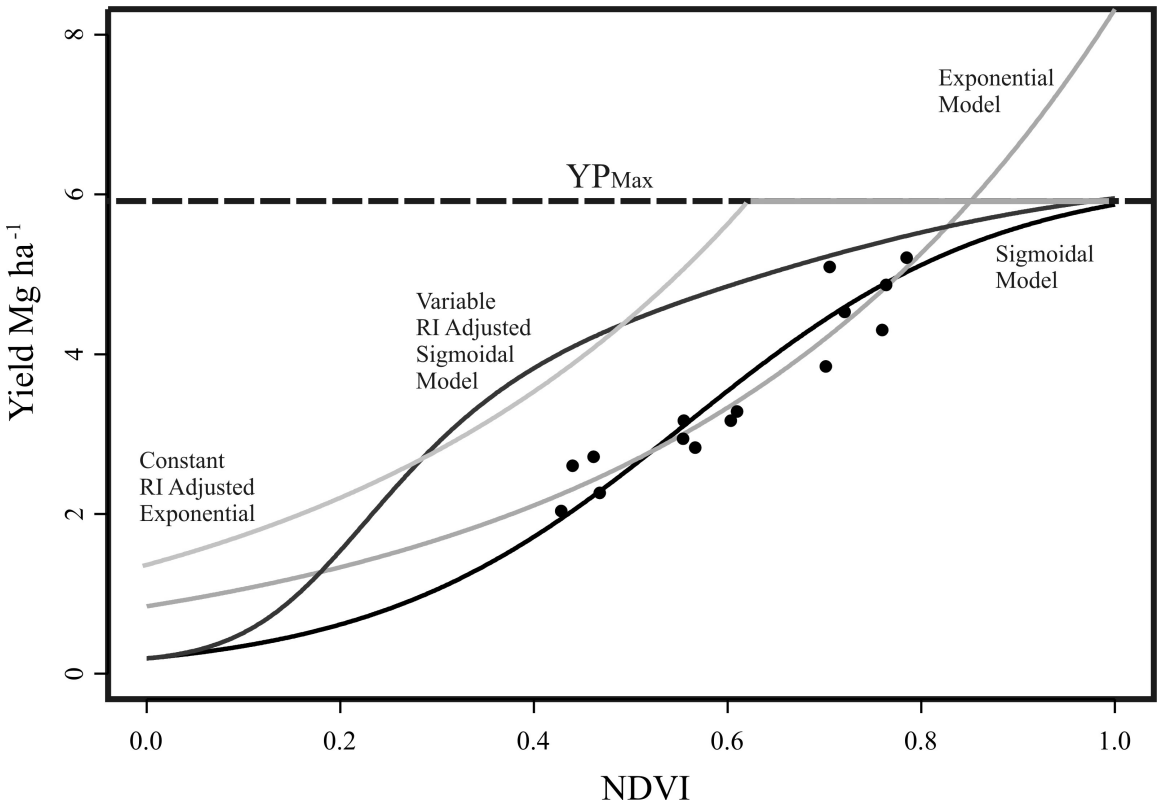

Figure 4.2: 1998 NDVI Verses Yield (Mg ha^{-1}) for 0 N pre-plant with Sigmoidal and Variable RI_{NDVI} Adjusted Models Compared to Exponential and Constant RI_{NDVI} Adjusted Models.

Figure 4.2 illustrates, due to continuously variable RI_{NDVI}, that the model shift is not only a rescaling but also a reformulation of the curve. To fit with preliminary assumptions, it is necessary that the RI_{NDVI} adjusted curve (YP_N) is asymptotic and that it approaches the non-RI_{NDVI} adjusted curve (YP_0) at extreme NDVI. It is also necessary that YP_N demonstrate variable response according to plant sensitivity to supplemental N.

Additionally, Figure 4.2 describes the marginal benefits of variable RI_{NDVI} adjustment of yield potential models. The constant RI_{NDVI} YP model (Equation 4.1) shows that marginal benefit (slope of the curve) increases at an increasing rate until YP_{Max} is reached and becomes zero thereafter. This implies that additional yield benefit of treating the next higher NDVI unit increases until YP_{Max}, but transitions to zero additional benefit after $YP_{Max.}$ The variable RI_{NDVI} adjusted YP model (Equation 4.2)

shows that marginal benefits increase at an increasing rate until the inflection point is reached and continues to increase thereafter but at a decreasing rate until YP_{Max} is reached. The combination of sigmoidal transition and variable RI_{NDVI} show that N supplementation will always result in an increase in yield; however, after the inflection point has been reached the additional benefit of treating the next unit of NDVI is smaller.

It should be noted that the dataset used to model the baseline sigmoidal curve was sensed at Feekes 4 –6 growth stage, while the RI_{NDVI} adjustment was an average of readings without specific growth stage from Monroe et al. (2008). Growth stage can influence the magnitude of maximum response, and will translate to the RI_{NDVI} adjusted yield model accordingly.

Monroe et al. (2008) also showed that differing definitions of bare soil NDVI (Ns) shift the response curve and can attenuate maximum response according to Equation 4.6

$$RI_{NDVI} = \begin{cases} 1 & \text{For NDVI} \le \text{Ns} \\ \dfrac{A_0(\text{FpNDVI} - \text{Ns})}{\cosh(A_1(\text{FpNDVI} - \text{Ns}))} + 1 & \text{For NDVI} > \text{Ns} \end{cases} \quad (4.6)$$

where RI_{NDVI} is 1 for NDVI definitions of bare soil greater than NDVI = 0. Figure 4.3 demonstrates how bare soil offsets are translated in the RI_{NDVI} adjusted curve (YP_N).

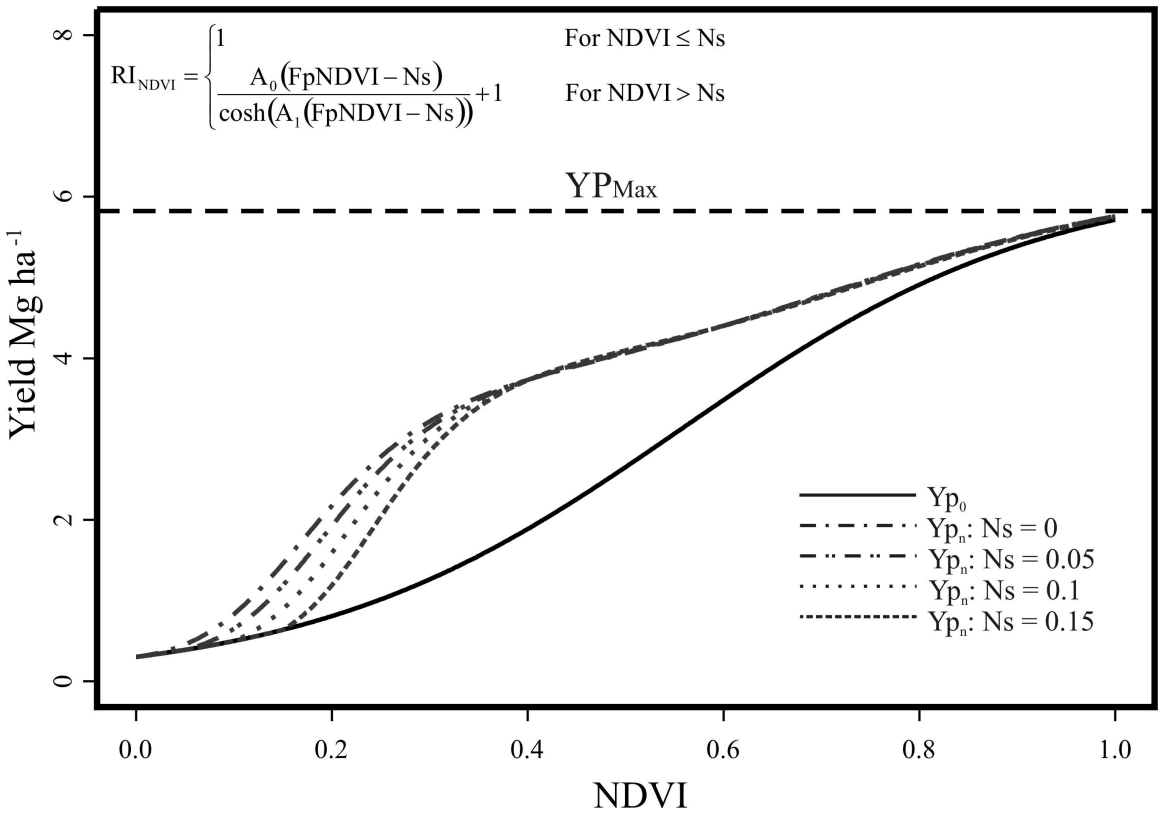

Figure 4.3: NDVI Verses the Variable RI_{NDVI} Adjusted Model in Yield (Mg ha^{-1}) with Various NDVI Definitions of Bare Soil (Ns = 0, 0.05, 0.1, and 0.15).

Figure 4.3 shows that as the definition of bare soil increases N enhanced yield (YP_N) remains equal to YP_0 until Ns ($RI_{NDVI} = 1$) is reached. After Ns is reached YP_N diverges from YP_0 according to the variable RI_{NDVI} model.

Monroe et al. (2008) suggest that RI_{NDVI} modeling parameters indicate the relative plant sensitivity to N supplementation. In general, for large RI_{NDVI} parameter values (A_0 and A_1 : Equation 4.2) plants are highly sensitive to N application for lower NDVI given by A_0 (maximum response); however, transition to sufficiency occurs at a much faster rate given by A_1 (transition rate). A high response to N for lower NDVI and a steep transition to sufficiency with increasing NDVI indicates that while N is a primary limiting factor for lower NDVI it is relegated to a subsidiary role as NDVI increases.

Conversely, lower parameter values generally indicate that N is consistently a main limiting factor. Figure 4.4 shows the sensitivity of YP_N shifted according variable RI_{NDVI} (Equation 4.2) parameters.

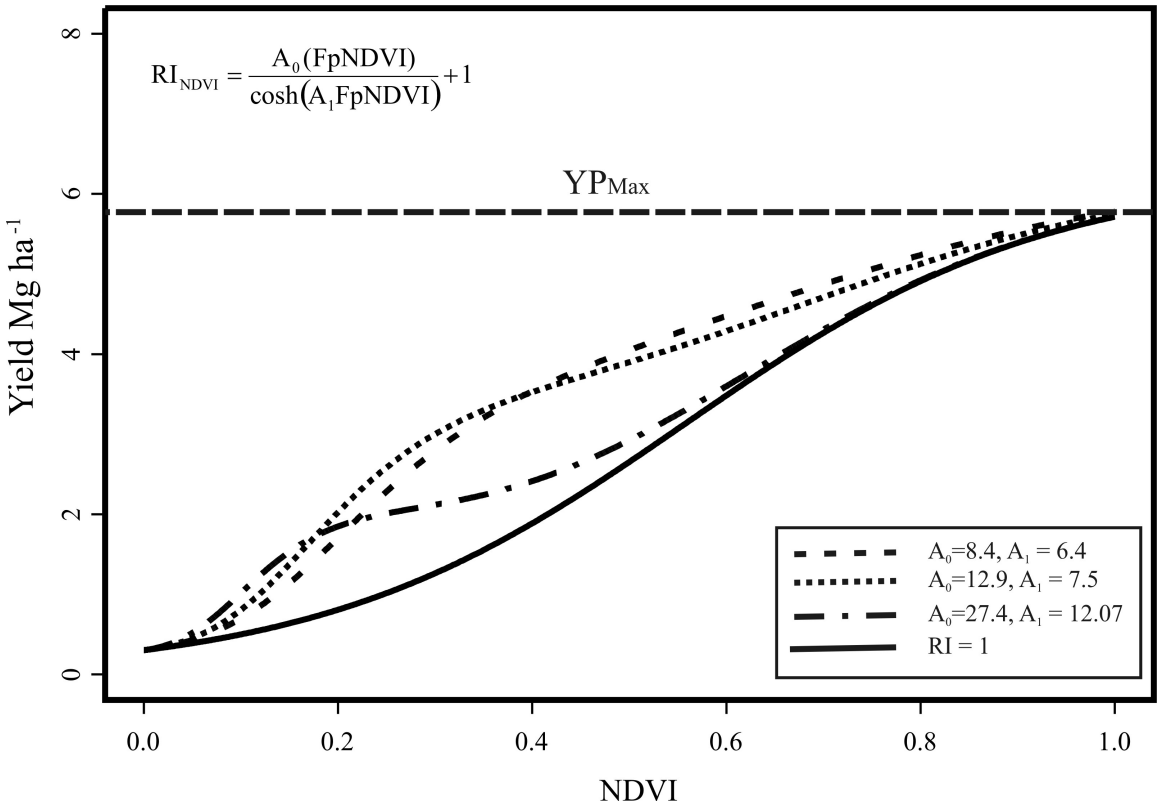

Figure 4.4: 1998 NDVI Verses Yield (Mg ha^{-1}) for 0 N pre-plant, with RI_{NDVI} Curve (Equation 4.2) Adjusted to Varying Parameters Monroe et al. (2008)

Figure 4.4 shows higher RI_{NDVI} parameters produce greater initial yield potential but quickly dissipate for higher NDVI. In this case, low NDVI is responsive to N supplementation but becomes insensitive quickly because yield sensitivity is based on residual N reserves not N supplementation. In these conditions, N is sufficient given physical/chemical limitations and denoted by steep transitions in RI_{NDVI} parameters. However, for lower RI_{NDVI} parameters (indicating consistent N sensitivity), onset yield potential is high and declines less across the NDVI spectrum. In these conditions, N

remains a primary limiting nutrient for more of the NDVI spectrum, and yield potential is a result of sufficiency through N supplementation.

Monroe et al. (2008) demonstrated RI_{NDVI} was also sensitive to N application rate. Figure 4.5 shows YP_N shifts for N applications of 22, 45, 67, 90, and 112 kg N ha^{-1} (20, 40, 60, 80, and 100 lbs N $acre^{-1}$) from the calibration stamp design using RI_{NDVI} parameter values shown in Table 4.2.

Table 4.2: N Application Rate RI_{NDVI} Adjusted Curve and Parameters.

N Rate (kg N ha^{-1})	A_0	A_1
112	4.84	5.71
90	6.76	6.78
67	3.36	5.78
45	3.91	6.41
22	4.37	10.33

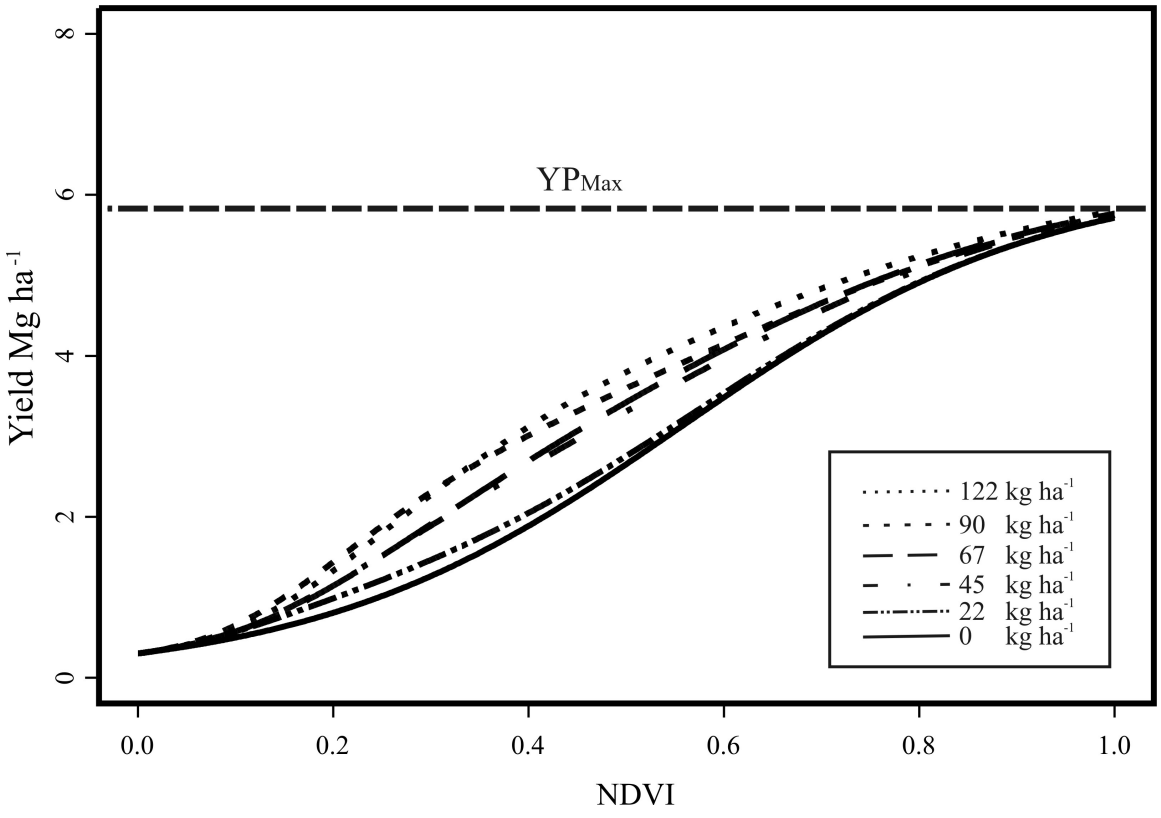

Figure 4.5: RI_{NDVI} Adjusted Curve for 22, 45, 67, 90, and 112 kg N ha^{-1} Application Rates.

Figure 4.5 demonstrates that reduced N application affects the YP_N curve in a predictable manner. As N application rate is reduced the net benefit (YP_N) is also reduced. This finding confirms Raun et al. (2005) statement that little yield is gained (net benefit of YP_N = 0.32 Mg ha^{-1}) from treatment above NDVI = 0.73 and findings in Monroe et al. (2008) showing that plant response to supplemental N is marginal (RI $\leq$ 10%) above NDVI = 0.73.

Subtracting baseline yield (YP_0) from N enhanced yield (YP_N) produces an estimate of yield gain due to N supplementation. Figure 4.6 shows the results of a methodology to derive net yield potential benefit from varied N application rates.

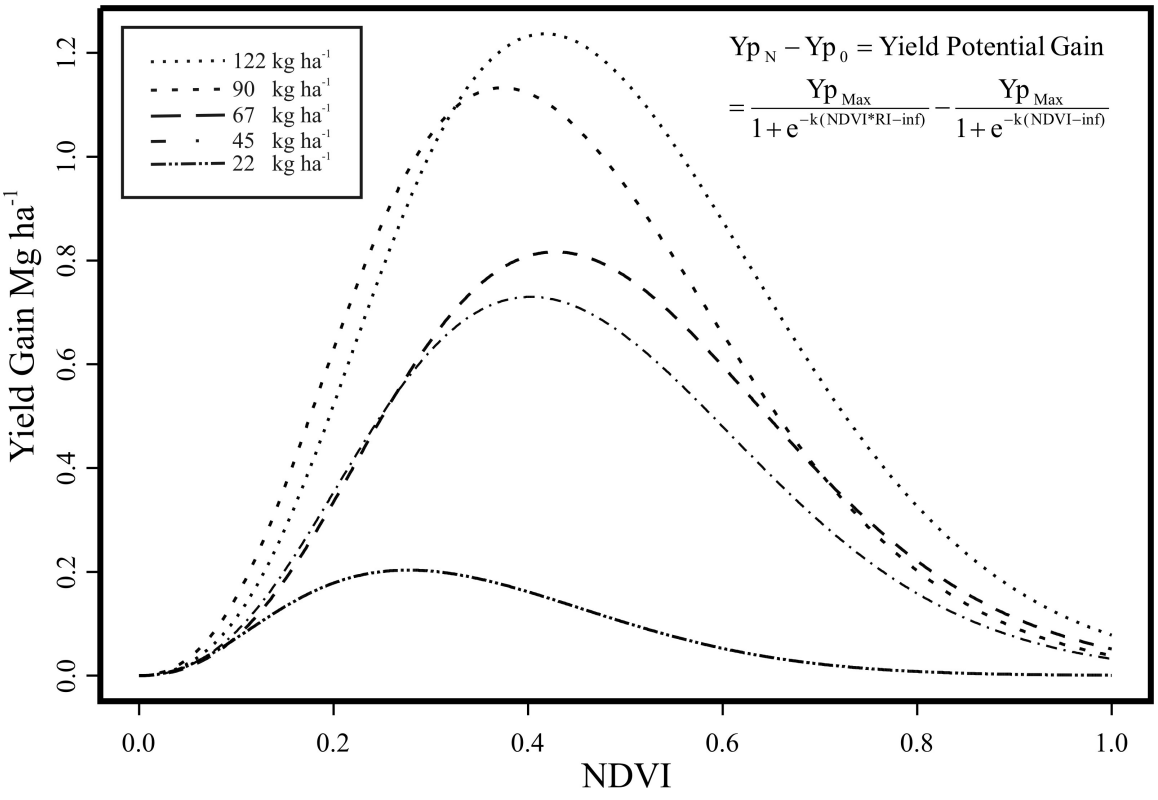

Figure 4.6: Yield Potential Gain Curve for 22, 45, 67, 90, and 112 kg N ha^{-1} Application Rates on Calibration Stamp Design Data.

Predictably, higher N application rates show greater yield potential gain across the NDVI spectrum. However, gain subsides for extreme NDVI. Figure 4.6 specifically shows the

interval of NDVI where yield is insignificantly altered due to increasing N application rates. The non-uniformity in the peaks of these curves is due to multiple wheat trials included in this experiment. Different fields have different responses to application rates of supplemental N.

Notably Raun et al. (2005) suggested, from empirical studies, that N application effects on yield gain would generally be unsubstantial for NDVI < 0.25, maximized between $0.25 \leq \text{NDVI} \leq 0.57$, decreasing for $0.57 < \text{NDVI} \leq 0.73$, and insignificant for NDVI > 0.73. Given the findings in Figure 4.6, these application intervals accurately describe this process. Given dynamic price changes in wheat and fertilizer prices this process can determine the net benefit of treating at higher N application rates to establish NDVI / N application rates.

Figure 4.7 demonstrates the effect of an alternate NDVI definition of bare soil (Ns) on yield gain (Equation 4.6). Specifically, Figure 4.7 shows the yield gain offset for the NDVI bare soil definition (Ns = 0.15).

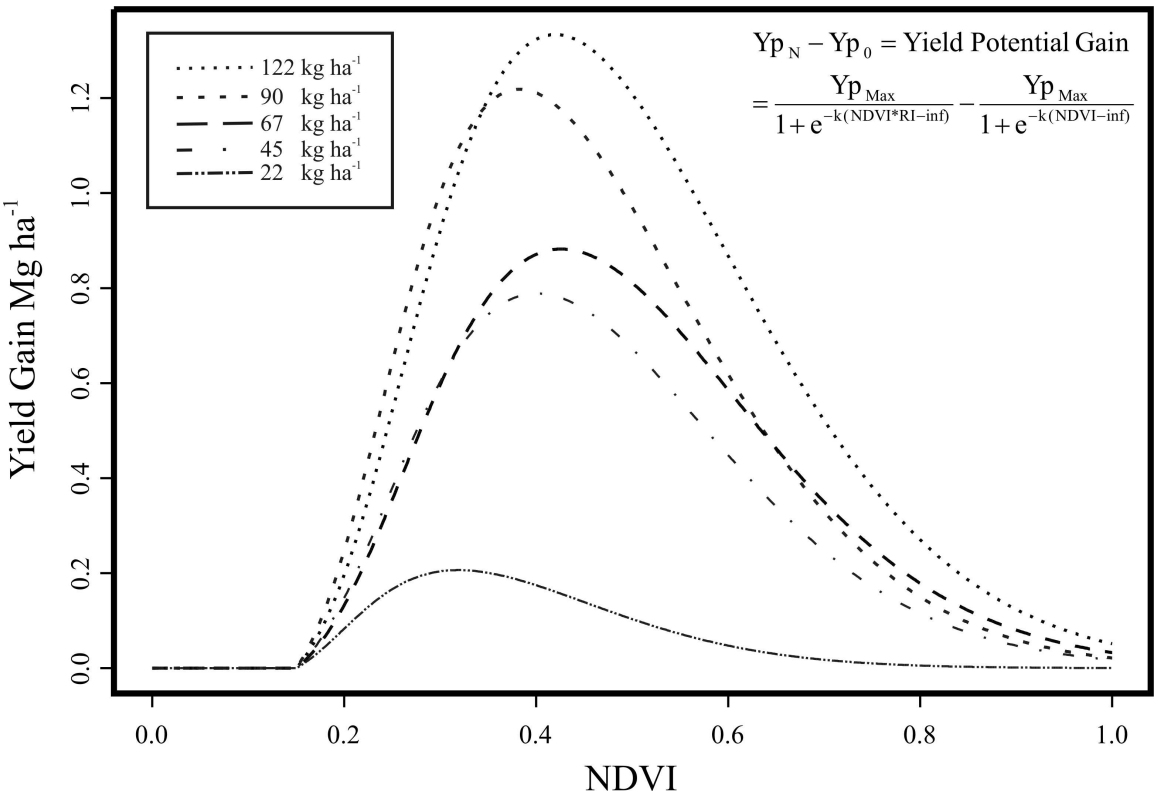

Figure 4.7: Yield Potential Gain Curve for 22, 45, 67, 90, and 112 kg N ha^{-1} Application Rates on Calibration Stamp Design Data Assuming the NDVI of Bare Soil (Ns) = 0.15 (Equation 4.6)

Predictably, allowing the definition of bare soil (Ns) to increase causes yield gain through N supplementation to be insignificant until Ns is reached. After Ns is reached differences in yield gain become apparent for each N application rate. Conceptually, regardless of application rate, N applied to bare soil will not cause a gain in yield because of a lack in plant material.

Conclusion

This research shows that a sigmoidal model estimates yield potential (YP_0) with the same relative accuracy as the Raun et al. (2005) exponential, but satisfies necessary asymptotic boundary conditions, such as $YP_0 \rightarrow 0$ for NDVI $\rightarrow$ 0 and $YP_0 \rightarrow YP_{Max}$ for NDVI $\rightarrow$ 1. A sigmoidal approach is also capable of continuously shifting due to the

influence of variable plant response to N supplementation (RI_{NDVI}) and coalescences YP_N and YP_0 at NDVI extremes.

This research also concluded a sigmoidal approach is capable of demonstrating variable physical/chemical conditions of plant sensitivity to N (RI_{NDVI}). The sigmoid model, incorporating the continuous variable (RI_{NDVI}) is able to adjust yield potential (YP_N) in response to conditions where N may not be the primary limiting nutrient.

Finally this study observed how YP_N in the sigmoidal approach responds to varied N application rates and shows boundaries of efficacious N supplementation, which could be used as an economic determiner of optimal NDVI / N application rate intervals.

References

Huang, W. 2007. Impact of rising natural gas prices on U.S. ammonia supply. Economic Research Service USDA. Report: WRS-0702. Available at: http://www.ers.usda.gov/publications/wrs0702

Johnson, G.V., W.R. Raun, and R.W. Mullen. 2000. Nitrogen use efficiency as influenced by crop response index. p.291. Agronomy Abstracts. ASA, CSSA, and SSSA. Madison, WI.

Johnson G.V., W.R. Raun. 2003. Nitrogen response index as a guide to fertilizer management. Journal of Plant Nutrition. Vol. 26. No. 2:249-262

Monroe, A.D., J.B. Solie, and W.R. Raun. 2008. Chapter 2. A continuous function to predict plant response to applied nitrogen. Unpublished Ph.D. dissertation.

Mullen R. W., K.W. Freeman, W. R. Raun, G. V. Johnson, M. L. Stone and J. B. Solie. (2003). Identifying an in-season response index and the potential to increase wheat yield with nitrogen. Agronomy Journal. 95:347-351.

Raun, W.R., J.B. Solie, G.V. Johnson, M.L. Stone, R.W. Whiney, H.L. Lees, H. Sembiring, and S.B. Phillips. 1998. Micro-variability in soil test, plant nutrient, and yield parameters in bermudagrass. Soil Science Society of America Journal. 62:683-690.

Raun W.R., J.B. Solie, M.L. Stone, D.L. Zavodny, K.L. Martin, and K.W. Freeman. (2004). Automated calibration stamp technology for improved in-season nitrogen fertilization. Agronomy Journal. 97:338-342.

Raun W.R., J.B. Solie, M.L. Stone , K.L. Martin, K.W. Freeman, R. Mullen, H. Zhang, J.S. Schepers, and G.V. Johnson. 2005. Optical sensor-based algorithm for crop nitrogen fertilization. Communications in Soil Science and Plant Analysis. 36:2759-2781.

Solie J.B., W.R. Raun, R.W. Whiney, S.L. Taylor, and J.D. Ringer. 1996. Optical sensor based filed element size and sensing strategy for nitrogen application. Transactions ASAE, 39. 6:1983-1992.

Solie J.B., W.R. Raun, and M.L. Stone. 1999. Submeter spatial variability of selected soil and plant variables. Soil Sci. Am. J. 63:1724-1733.

Tsoularis, A. and J. Wallace. 2002. Analysis of logistic growth models. Mathematical Biology. Vol 179. No.1:21-55.

CHAPTER V

CONCLUSIONS

CHAPTER 2

The objective of Chapter 2 was to reexamine constant response index at fine resolution. Chapter 2 demonstrates that plant response to supplemental N (RI_{NDVI}) is continuous, variable, and should be modeled using a peak function. Predicting RI_{NDVI} in this manner fits the data distribution and conforms to necessary boundary conditions. Conceptually, plant response should not be observable for low NDVI because of the scarcity of plants. Increasing NDVI (i.e. more plants) will exhibit greater response so long as N remains a limiting factor. As residual N increases (with increasing NDVI) plant response to supplementation decreases, and finally as residual N reaches sufficiency plant response to supplementation becomes insignificant.

This study also showed that there is a necessity to modify initial boundary conditions (RI_{NDVI} =1 at NDVI =0) to account for the influence of bare soil NDVI on response. This was accomplished by adding a bare soil NDVI (Ns) definition that adjusts the peak function.

The zone of maximum response to supplementation determines the interval and magnitude of the highest N limitation. The rate of transition from maximum response to N sufficiency describes the relative importance of N as a limiting nutrient and is site- and species-specific. Complete N sufficiency is reached when supplementation no longer causes a significant response. Using this information to optimize plant response N should be applied conservatively to extremes in NDVI, namely between 0 < FpNDVI <

maximum response and FpNDVI > N sufficiency. This research also suggests that N be applied proportionally on the interval maximum response < FpNDVI < N sufficiency.

CHAPTER 3

The goal of Chapter 3 was to establish an equitable method of determining fraction of vegetative cover (FVC) using a combination of relationships found in the literature and sensor technology. Chapter 3 shows that a combination of optical sensors capable of sub-sampling and spectral mixture analysis has the potential of accurately predicting FVC. Sensors capable of sub-sampling within an experimental area (pixel or plot) are able to determine variance. This research shows that within experimental area NDVI variance is quadratically related to mean NDVI, such that variance is low for pure regions (bare soil or complete vegetation). This research also shows that within experimental area NDVI variance is maximized at 50% coverage, such that variance is greatest when there is a near equal mixture of bare soil and complete vegetative cover within a sub-sample. This research concludes that a quadratic relationship exists between within experimental area variance and NDVI and within experimental area variance and FVC implying a predictable linear relationship exists between FVC and NDVI. This linear relationship, albeit found by other methods, is confirmed in the literature.

CHAPTER 4

The goal of Chapter 4 was to incorporate variable plant response to N supplementation with findings from current research under imposed conceptual boundary conditions to predict yield potential. Previous research in yield potential prediction found that yield was insignificant for low NDVI, increased exponentially through mid-range NDVI, and is constrained under a bio-physical cap for high NDVI. It has also been

shown that yield for low NDVI could be shifted to the bio-physical cap quicker by N supplementation. This shift is accounted for by a constant multiplier in the current yield potential prediction model. Chapter 4 showed that current methodology could be improved using a sigmoidal model, which asymptotically predicts low yield for low NDVI, is exponentially related to yield through mid-range NDVI, and asymptotically converges to the bio-physical cap (YP_{Max}) for high NDVI. Chapter 4 further demonstrated a methodology for incorporating variable plant response to N, which dynamically shifts the yield prediction curve to the bio-physical cap in accordance with plant sensitivity. This finding was then used to develop a method of determining yield gain under N application.

GENERAL FINDINGS

The object of this dissertation was to quantify supplemental N need and develop methodology to limit N application to areas not in need, thus minimizing over application and thereby creating a positive environmental externality. The findings from this research show that continuously variable plant response to N can define need, given field variability. Variable plant response in conjunction with a continuous sigmoidal yield potential relationship, which incorporates boundary conditions, can be used to predict economically optimal N application intervals on the normalized difference vegetative index (NDVI). Further, this research proposes that sigmoidal yield prediction, sensitive to variable plant response, combined with economic methods should be able to determine maximum application rates within optimal NDVI intervals. Thus Nitrogen supplementation to areas of need at economically optimized rates should produce environmentally responsible practices.

FURTHER RESEARCH

1. The design structure, using calibration stamp methodology, in this dissertation was originally intended to determine the stationarity of variable RI across a farm field using stratified random sampling. However, because distance dependency played little part in developing the variable RI relationship, no further work was completed in this area. Further research should be conducted to determine if the variable RI relationship exhibits field level stationarity.
2. This research found that fractional vegetative coverage (FVC) could be estimated using optical sensors capable of sub-sampling and provided a methodology relating NDVI to FVC. Current research in the literature suggests that FVC is related to yield; however, this research did not find a useful relationship between FVC and yield potential, although a connection should intuitively exist. Further experimentation may demonstrate FVC as providing ancillary information to aid in yield potential modeling.
3. Chapter four used an iterative process along with non-linear regression to fit sigmoidal model parameters. However, the bio-physical cap (YP_{Max}) was iteratively fit outside the regression model, and specified such that the sigmoidal model reached YP_{Max} at NDVI = 1. Further research should be conducted to either: 1. Quantify a model describing YP_{Max} from the biological or physical controlling factors, or 2. Derive a method of iteratively estimating YP_{Max} from yield dataset.

APPENDICIES

The following sections describe data collection and processing, field methodology, and experimental designs use in this dissertation. In addition, there is an equations section for the equations found in the literature and equations derived for this research.

Section A1 outlines the extraction of N-Rich strip data from IKONOS imagery, first order geographic search algorithm, and post-processing methods. Section A2 describes fieldwork and collected samples under the calibration stamp design. Additionally, there is an overview of variogram directed stratified random sampling used to maximize spatial relatedness between calibration stamps. Section A3 lists the equations found in the literature and author names. Section A4 lists the derived equations used in this study. Not all derived equations were directly used in this dissertation; specifically the derivatives and anti-derivative of the continuous RI_{NDVI} model were used to test continuity and limits at boundary conditions but were not listed in those respective chapters. They are listed here for future reference. Section A5 contains secondary reference material useful to this dissertation, specifically derivation of equations and statistical design. These references are included for further research.

A1: SATELLITE DATA ACQUISITION AND PROCESSING

In the preliminary portion of this project six fields were selected from satellite imagery where Oklahoma State University Department of Plant and Soil Science placed non-limiting nitrogen (N-rich) strips in operative farm fields. The six fields were covered in two successive IKONOS (4 m spatial resolution) images captured on June 25th 2002. One image contained five fields while the other field was part of the second image for the same acquisition date, thus minimizing inter-imagery differences in spectral resolution. The images were converted to normalized difference vegetative index (NDVI) images using the standard NDVI relationship

$$\mathrm{NDVI} = \frac{\mathrm{Nir} - \mathrm{Re\,d}}{\mathrm{Nir} + \mathrm{Re\,d}} \qquad \text{(A1)}$$

where Nir is the near-infared band (800 ± 50 nm) and Red is the red band (660 ± 40nm). All data inconsistencies, such as NDVI < 0, were reallocated to NDVI = 0 to maintain computation integrity.

N-Rich strips were identified by higher ambient NDVI, masked from the general dataset, and held over in vector format for later processing. Pixel allocation was constructed by drawing a line through the center of the N-Rich strip and extending a buffer zone 30 ft perpendicular to the direction of travel, which coincides with the 60 ft span of the applicator used to top-dress nitrogen.

This design is a pairwise NDVI comparison between elements in the strip (SpNDVI) and adjacent farmer practice elements (FpNDVI). Figure A1 shows the allocation of spatial neighbors and comparisons for satellite data.

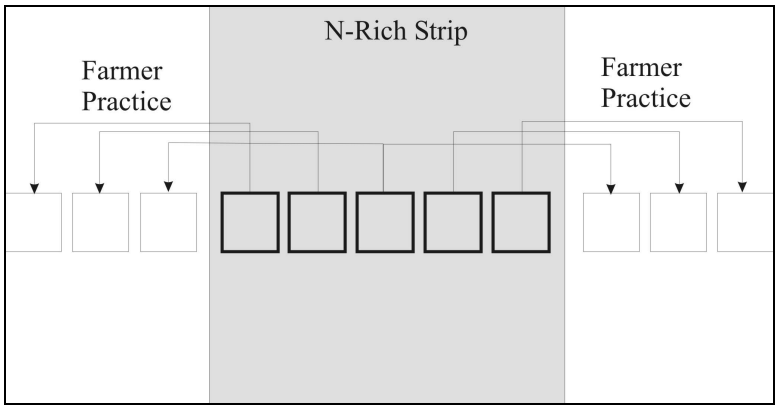

Figure A1: Pairwise Pixel Allocation for N-Rich Strip and Farmer Practice Strips in IKONOS Imagery

Figure A1 shows that idealized paired comparison allocation, where pixels within the strip are paired with immediate pixels outside the strip. The number of pixels in the strip zone is a function of the strip width, spatial alignment of the satellite image to strip direction, and the image resolution. The computational method of determining nearest neighbors was based on orthogonal first order choice algorithm, in which element pairs are chosen based on being aligned perpendicular to the direction of the N-rich strip and under a specified search radius.

Table A1 shows the variable list as it processed by array name.

Table A1: Array variable name and location for each IKONOS scanned farm.

Array Name	Name
Set 1	Bens
Set 2	Cassidy
Set 3	Roberts
Set 4	McCoy
Set 5	Peter's Home
Set 6	Spencer
Combined	All Data Sets

A2: FIELD WORK AND CALIBRATION STAMP ALLOCATION

The calibration stamp described in Raun et al (2005a) is a 9-square meter application of nitrogen (solution 32) over a 3 by 3 matrix of one-meter square elements. Figure A2, shows the basic outline and design of the calibration stamp.

FP 1	NA 40	FP 4
NA 20	NA 100	NA 60
FP 2	NA 80	FP 3

Figure A2: N Application Routine for Calibration Stamp Design. Each Element is 1m^2 in Area.

Five elements receive progressive amounts of nitrogen 22, 45, 67, 90, and 112 kg N ha^{-1} (20, 40, 60, 80, and 100 lbs N acre^{-1}) denoted by (NA 20 – 100) and four elements that receive no nitrogen plot (FP 1 – 4).

The cell size of the calibration stamp is a compromise between work performed by Solie et al. (1999), where semivariance analysis showed effective ranges between 1.04m and 6.70m for total extractable P,K, organic C, and pH and the dimensions that could reasonably be used based on equipment designed for this task. The design of the calibration stamp therefore maximizes the within stamp spatial correlation.

Several calibration stamps (167) were placed on five fields in the Payne County, OK. on small non-committed plots at Oklahoma State University's research stations across two plant species (winter wheat and bermudagrass). Two calibration stamp experiments were applied to winter wheat in experimental areas. Three were placed in native bermudagrass stands. Because of the mixture of species timing was factored out as a blocking variable. Repeated measures were taken of the winter wheat to assess the best relationship between nitrogen application and NDVI. Bermudagrass measures were preformed during the peak of the growing season.

It was necessary to distribute the stamps in field based on a stratified random sampling method to prevent preferential clustering of data. In previous works, it has been observed that an autocorrelation relationship exists between samples (NDVI, soil, etc.) in close spatial proximity. Work by Kerry and Oliver (2003) showed that soil samples could be allocated in strata and variation could be preserved when sample intervals were set at half the observed variogram range. The variograms, in this case, were based aerial photography of the field. Prior studies by McBratney and Pringle (1997, 1999) show that for fields with no recorded data, variograms could be constructed by taking the average of variograms; this was cited in Kerry and Oliver's (2004) later studies. It was determined to use prior information to direct the layout of the calibration stamp design.

The six IKONOS images were geostatistically analyzed and average NDVI semi-variogram was constructed. From this an effective range was detailed that would determine the spatial spread between calibration stamps. Figure A3 shows the average semi-variogram structure.

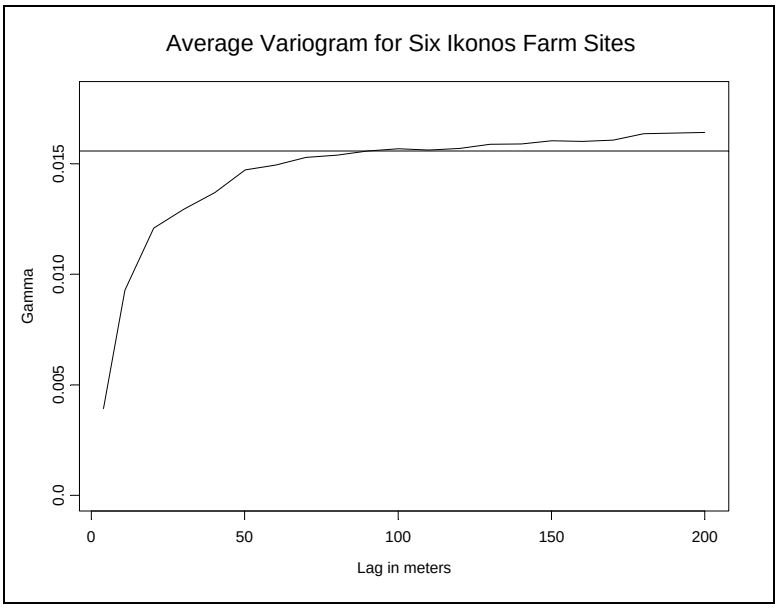

Figure A3: Average Variograms for the Six IKONOS Farm Sites

Figure A3 shows that approximately 90m-separation distance between samples tends to intersect with the average of the population variance (gamma ≈ 0.0152). Spatial lags below this intersection point exhibit spatial dependence.

The calibration stamps were distributed across the five field sites by constructing strata where the diagonal distance of the strata was set to one-half the average variogram range (45m) of the six fields captured with IKONOS imagery.

Figure A4 shows an example layout for four successive strata.

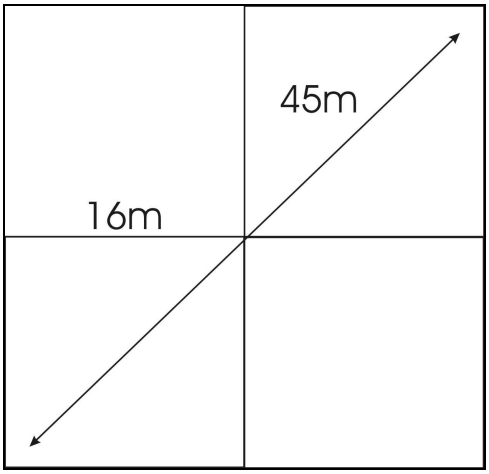

Figure A4: Maximum Offset Distance Between Two Calibration Stamps. Each Sampling Strata is 16m x 16m.

A calibration stamp was placed in each strata where the maximum distance between stamps of any two strata (s) is $0\text{m} \leq D(s_i, s_j) \leq 45\text{m}$. This allocation of rectangular strata was applied to each field. This methodology neglected boundary or edge effects where strata arrangement may have overlapped field boundary. Edge effects were removed by only selecting to apply calibration stamps in strata containing 240 m^2 area.

The location of the stamp within each stratum was determined by a random uniform coordinate generator that selected northing and easting coordinates independently. The locations were then downloaded to GPS location device, marked in the field, and a stamp was applied.

Since the calibration stamp configuration could not be randomized in-field and was always as described as in Figure A2, it was necessary to randomly assign travel direction to each calibration stamp location to remove directional bias. A randomized value (0 – 3608) was determined by a random uniform generator and measured in-field by magnetic compass. Additionally, two fields received a multi-stamp where three successive calibration stamps were placed end to end. This modification in the experimental design was made to increase sample size and to better simulate an N-Rich

strip. For this design it was more important to randomize direction of travel to remove preferential direction bias.

The calibration stamps were remotely sensed two weeks after application with the Greenseeker™ handheld optical crop sensor described in (Solie et al. 2002). The Greenseeker™ is radiometric sensor that pulses red (660nm) and near infrared (780nm) light through a battery of light emitting diodes. The pulsed light is detectable from background radiation, which eliminates the need for a secondary upward pointing sensor to distinguish between produced signal and ambient sunlight. For this experiment the Greenseeker™ was used to calculate an average NDVI reading for each element of the calibration stamps place in field.

Table A2: Data set name, species of plant, sampling routine, and location for each field trial.

Name	Species	Samples	Location
Monroe	Bermudagrass	Repeated (2)	East of Perkins
Perkinst	Bermudagrass	Single	Perkins Station
Efaw	Bermudagrass	Single	Efaw testing West of Stillwater
Perkins	Wheat	Repeated (4)	Perkins Station
Black	Wheat	Repeated (3)	Lake Carl Blackwell

Sampling sessions were either temporal replicates or single replicates. Three fields had repeated measures to determine the best time for sensing, while two fields had single sampling with extended calibration stamp application.

The following table shows the sampling date of each temporally repeated measure at each site.

Table A3: Data set name, sensing date, species, and design for each of the field trials.

Name	Date	Species	Trial
Blackwell	2/23/2004	Winter Wheat	Temporal Reps
Blackwell	3/21/2004	Winter Wheat	Temporal Reps
Blackwell	3/28/2004	Winter Wheat	Temporal Reps
Blackwell	4/4/2004	Winter Wheat	Temporal Reps
Perkins	2/18/2004	Winter Wheat	Temporal Reps
Perkins	3/21/2004	Winter Wheat	Temporal Reps
Perkins	3/29/2004	Winter Wheat	Temporal Reps
Monroe	7/14/2004	Bermudagrass	Temporal Reps
Monroe	8/17/2004	Bermudagrass	Temporal Reps
Perkstation	8/10/2004	Bermudagrass	Single Repeated
Efaw	6/24/2004	Bermudagrass	Single Repeated

Originally, Perkins (perk) was sampled a total of four times on or near the date Blackwell (black) was sampled. However, issues with the data from this sample made it usable for this project.

For each calibration stamp element soil samples were collected and analyzed. Nine soil cores per element were collect at approximately 15cm depth and composited. Chemical analysis was recorded for soil pH (pH), initial NO_3 levels (NO_3), phosphorus (P), potassium (K), and electro-conductivity (EC). Table A4 shows the coefficient of determination for a regression model of NDVI at 112 kg N ha^{-1} (SpNDVI) on non-treated NDVI (FpNDVI) with chemical covariates.

Table A4: Soil test parameters used as covariates to determine relative increase in predication potential.

Names	Dates	Standard Model	pH	NO_3	P	K	EC
monroe	7/14/2004	0.701	0.715	0.702	0.705	0.701	0.727
monroe	8/17/2004	0.516	0.516	0.532	0.516	0.518	0.52
perkst	8/10/2004	0.45	0.47	0.45	0.463	0.458	0.451
efaw	6/24/2004	0.546	0.547	0.546	0.551	0.569	0.546
black	2/23/2004	0.728	0.728	0.728	0.731	0.755	0.73
black	3/21/2004	0.601	0.608	0.601	0.601	0.608	0.603
black	3/28/2004	0.763	0.764	0.783	0.772	0.798	0.766
black	4/4/2004	0.855	0.859	0.855	0.858	0.855	0.862
perk	2/18/2004	0.724	0.737	0.724	0.758	0.725	0.724
perk	3/21/2004	0.624	0.63	0.625	0.634	0.625	0.627
perk	3/29/2004	0.601	0.602	0.601	0.602	0.646	0.602

In Table A4 Standard Model is the R^2 of the base model without covariates. Table A4 shows that there is little increase in explained variation by adding soil covariates.

A3: EQUATIONS FROM LITERATURE

Coefficient of Variation

$$CV = 100\left(\frac{S_x}{\bar{x}}\right)$$

FVC – Predicted percent vegetative cover (Gutman and Ignatov 1998)

$$FVC(N) = \frac{N - N_s}{N_c - N_s}$$

N = observed NDVI
N_s = NDVI of endmember for bare soil
N_c = NDVI of endmember complete plant coverage

NDVI – Normalized Difference Vegetative Index (Reflectance)

$$NDVI = \frac{NIR - Red}{NIR + Red}$$

RSS – Residual Sum of squares

$$RSS = \sum (y - \hat{y})^2$$

$RI_{Harvest}$ – Response Index Harvest (Johnson et al. 2000)

$$RI_{Harvest} = \frac{\text{Yield (Treated plot)}}{\text{Yield (Check plot)}}$$

RI_{NDVI} – Response Index from NDVI (Mullen et al. 2003)

$$RI_{NDVI} = \frac{\text{NDVI (Treated)}}{\text{NDVI (check)}}$$

RI_{NDVI} –Equation from Yield Potential (Raun et al. 2005b)

$$RI_{NDVI} = \begin{cases} \dfrac{YP_N}{YP_0} & \text{for } YP_N < YP_{Max} \text{ and NDVI} > 0.25 \\ \dfrac{YP_{Max}}{YP_0} & \text{for } YP_N \geq YP_{Max} \text{ and NDVI} \leq 0.73 \\ 1 & \text{for } YP_0 \rightarrow YP_{Max} \text{ and NDVI} > 0.73 \end{cases}$$

Spectral Mixture model (SMA) – (Gutman and Ignatov 1998)

$$NDVI = FVC(N_c) + (1 - FVC)N_s$$

Yield Potential Model – (Raun et al. 2005b)

$$YP_N = a(RI_{NDVI})e^{b(NDVI)} \quad \text{for:} \quad YP_N < YP_{Max}; RI_{NDVI} = 1 \text{ for } N = 0$$

A4: DERIVED EQUATIONS

Satellite data filter

$$Mean_{(SpNDVI \pm FpNDVI)} \pm 3.5S_{(SpNDVI \pm FpNDVI)}$$

RI_{NDVI}(FpNDVI) –RI prediction model

$$RI_{NDVI} = \frac{A_0(FpNDVI)}{\cosh(A_1 FpNDVI)} + 1$$

RI_{NDVI}(FpNDVI) –RI prediction model with bare soil NDVI (Ns) correction

$$RI_{NDVI} = \begin{cases} 1 & \text{For NDVI} \leq Ns \\ \dfrac{A_0(FpNDVI - Ns)}{\cosh(A_1(FpNDVI - Ns))} + 1 & \text{For NDVI} > Ns \end{cases}$$

RI_{NDVI}`(x) – First derivative of the RI model

$$RI_{d1}(x) = L\left(\frac{1}{\cosh(Ax)} - \frac{Ax\sinh(Ax)}{\cosh^2(Ax)}\right) = L\left(\frac{\cosh(Ax) - Ax\sinh(Ax)}{\cosh^2(Ax)}\right)$$

$RI_{NDVI}``(x)$ – Second derivative of the RI Model

$$RI_{d2}(x) = L\left(\frac{2A^2x\sinh^2(Ax) - A^2x\cosh^2 Ax - 2A\sinh(Ax)\cosh(Ax)}{\cosh^3(Ax)}\right)$$

$\int RI_{NDVI}(x)$ = Anti-derivative of RI model

$$\int RI_{NDVI} = \frac{L\tan^{-1}(e^{Ax})}{A} + x$$

Sigmoidal Prediction Model: YP at 0 N application

$$YP_0(NDVI) = \frac{YP_{Max}}{1 + e^{-k(NDVI - inf)}}$$

Sigmoidal Prediction Model: YP with N application

$$YP_N(NDVI) = \frac{YP_{Max}}{1 + e^{-k(NDVI*RI - inf)}}$$

A5: SECONDARY SOURCE MATERIAL

This section contains citations not used in the dissertation but useful to experimental design, citations of equations and relationships in the appendices, and citations useful in pursuing further research dealing with this dissertation.

Gutman, G. and A. Ignatov. 1998. The derivation of the green vegetation fraction from NOAA/AVHRR data for use in numerical weather prediction models. International Journal of Remote Sensing. Vol. 19. No. 8. Pgs 1533-1543.

Kerry, R. and Oliver M.A. 2003. Variograms of Ancillary Data to Aid Sampling for Soil Surveys. Precision Agriculture. 4:253-270

Kerry, R. and Oliver M.A. 2004. Average Variogram to Guide Soil Sampling. International Journal of Applied Earth Observation. 5:307-325.

McBratney, A.B. and Pringle, M.J. 1997. Spatial Variability in Soil Implications for Precision Agriculture. In: Stafford, J.V. Precision Agriculture 1997 vol. 1. BIOS Scientific Publishers, Oxford, pp 3-31.

McBratney, A.B. and Pringle, M.J. 1999. Estimating average and proportional variograms of soil properties and their potential use in precision agriculture. Precision Agriculture. 1:125-152.

Mullen, R.W, K.W. Freeman, W.R. Raun, G.V. Johnson, M.L. Stone, and J.B. Solie. 2003. Identifying an In-Season Response Index and the Potential to Increase Wheat Yield with Nitrogen. Agronomy Journal 95:347-351.

Johnson, G.V., W.R. Raun, and R.W. Mullen. 2000. Nitrogen Use Efficiency as Influenced by Crop Response Index.. p. 291. In Agronomy Abstracts. ASA, CSSA, and SSSA, Madison, WI.

Raun, W.R., J.B. Solie, M.L. Stone, D.L. Zavodny, K.L. Martin, and K.W. Freeman. 2005a. Automated calibration stamp technology for improved in-season nitrogen fertilization. Agronomy Journal 97:338-342.

Raun, W.R., J.B. Solie, M.L. Stone, K.L. Martin, K.W. Freeman, R.W. Mullen, H. Zhang, J.S. Schepers, and G.V. Johnson. 2005b. Optical sensor-based algorithm for crop nitrogen fertilization. Communications in Soil Science and Plant Analysis. 36: 2759-2781.

Solie, J.B., M.L. Stone, W.R. Raun, G.V. Johnson, K. Freeman, R. Mullen,D.E. Needham, S. Reed, and C.N. Washmon. 2002. Real-time sensing and N fertilization with a field scale Greenseeker applicator. Accessed on-line on 1/28/2007 at: http://nue.okstate.edu/Papers/Minnesota_2002_Solie.htm

Solie, J.B., W.R. Raun, and M.L. Stone. 1999. Submeter spatial variability of selected soil and plant variables. Soil Science Society of America Journal. 63:1724-1733.

VITA

Alvin Dean Monroe, Jr

Candidate for the Degree of

Doctor of Philosophy

Dissertation: NORMALIZED DIFFERENCE VEGETATIVE INDEX BASED CROP YIELD PREDICTION MODELS TO MINIMIZE NITROGEN FERTILIZER APPLICATION

Major Field: Environmental Science

Biographical:

Personal Data: Born February 7th 1975 in Chickasha Oklahoma to Alvin D. and Patsy S. Monroe, Sr.. Residences in Konawa (1976 – 1999) and Perkins (2001 – 2008), Oklahoma.

Education:

Graduated from Konawa High School, Konawa Oklahoma 1993, earned a Bachelors of Science in Cartography in 1999 from East Central University, Ada Oklahoma, and earned a Masters of Science degree in Geography in 2001 from Oklahoma State University, Stillwater Oklahoma. Completed the requirements for a Doctorates degree in Environmental Science from Oklahoma State University December 2008.

Experience:

Professional Cartographer with the Environmental Protection Agency and Bureau of Census 1996 – 1999, and 2000, respectively. Part time teaching and research assistant with Oklahoma State University in Departments of Geography 1999 - 2001 and Biosystems and Agricultural Engineering 2002 - 2008. Adjunct professor of Mathematics at Northern Oklahoma College 2005 – current.

Professional Memberships: Sigma Xi, American Association of Geographers, and American Association of Agricultural and Biological Engineers.

Name: Alvin Dean Monroe, Jr Date of Degree: December 2008

Institution: Oklahoma State University Location: OKC or Stillwater, Oklahoma

Title of Study: NORMALIZED DIFFERENCE VEGETATIVE INDEX BASED CROP YIELD PREDICTION MODELS TO MINIMIZE NITROGEN FERTILIZER APPLICATION

Pages in Study: 92 Candidate for the Degree of Doctor of Philosophy

Major Field: Environmental Science

Scope and Method of Study: The purpose of this study was to develop a theoretical basis and numerical strategy to optimize nitrogen (N) fertilizer application and thereby improve crop yield potential models, increase economic efficiency, and reduce excess N entering the environment. This study focused on formulating systematic continuous functions to describe the relationship between plant response to supplemental N fertilizer and spectral measures of plant stand quality (normalized difference vegetative index or NDVI). A derived continuous definition of plant response to N was combined with current agronomic theory to extend current yield potential modeling equations. Secondary research in this study evaluated the estimation and use of fractional vegetative cover as an ancillary description of yield.

Findings and Conclusions: This study found that plant response to supplemental nitrogen (N) is functionally related to plant stand quality and residual N sufficiency measured by NDVI. Specifically plant response to supplemental N decreases as plant stand quality increases as a function of residual N from the plant-soil matrix. A sigmoidal yield equation was proposed to replace existing yield potential models, which incorporated agronomic boundary conditions and continuous plant response to supplemental N. This study demonstrated that the sigmoidal yield curve integrated continuous plant response to N supplementation and biological constraints more effectively than current empirically derived models. Additionally, the sigmoidal model demonstrated a method of predicting the maximum biophysical limit of yield and provided a quantifiable estimate of yield gain. Furthermore, yield gain was found to be subject to N application rate and further research could be developed to derive the economic net benefit of application rate for specific plant stands. Secondary research in this study also found that fractional vegetative cover could be estimated by a systematic relationship between the mean and variance of NDVI measured by sub-sampling sensors. This finding did not directly contribute to yield prediction, but provides an applicable method for estimating fractional vegetative cover in the field with the use of sub-sampling optical sensors.

ADVISER'S APPROVAL: Dr. John B. Soile